Leveraging Synthetic Lethality in Triple-negative Breast Cancer with Inhibited Eukaryotic Initiation Factor-4E Phosphorylation

By Qiyun (Catherine) Deng

Department of Biochemistry

McGill University, Montreal

A thesis submitted to McGill University in partial fulfillment of the requirements for the degree of Master of Science in Biochemistry

Abstract

While significant advancements have been made in breast cancer treatment, the most aggressive form, Triple-Negative Breast Cancer (TNBC), remains challenging to treat due to its lack of the three well-established breast cancer drug targets. For the cancer cells to proliferate and metastasize, mRNA translation must be altered to adapt to different cellular cues. Therefore, therapies targeting mRNA translation represent a promising anti-cancer strategy, and numerous drugs have been developed to target the translation initiation machinery. A key regulator of translation initiation is the mRNA cap-binding protein, eukaryotic initiation factor 4E (eIF4E). Phosphorylation of eIF4E by MNK1/2 [MAPK (Mitogen-Activated Protein Kinase)-Interacting Kinase 1/2] promotes tumorigenesis by enhancing the translation of a specific subset of mRNAs encoding critical proteins for cell survival and metastasis. Our lab previously demonstrated that the loss of phospho-eIF4E (p-eIF4E) significantly limits TNBC metastasis but does not affect primary tumor growth. Although monotherapy is still the common approach for treating cancer, combination therapy has become more prominent because cancer cells have lower chances of developing multiple drug resistance. Thus, this project aims to find a novel combination therapy targeting both TNBC primary tumor growth and metastasis. To this end, synthetic lethal partners of p-eIF4E were investigated by performing an unbiased genetic screen using an MNK1/2 inhibitor (eFT508) in a TNBC cell line, MDA-MB-231. Through statistical analyses and target validation using short hairpin RNAs (shRNAs) and small-molecule inhibitors, we identified the inhibition of cyclin-dependent kinase 4 (CDK4) by Palbociclib, a CDK4/6 inhibitor, showed strong synergy with eFT508 treatment. This finding suggests that the combination therapy of MNK1/2 and CDK4 inhibitors might be beneficial for treating TNBC metastasis and primary tumor simultaneously, providing a new therapeutic approach in TNBC targeted therapies.

Résumé

Bien que des progrès significatifs aient été réalisés dans le traitement du cancer du sein, la forme la plus agressive, le cancer du sein triple négatif (TNBC), reste difficile à traiter en raison de l'absence des trois cibles médicamenteuses bien établies contre le cancer du sein. Pour que les cellules cancéreuses prolifèrent et métastasent, la traduction de l'ARNm doit être modifiée pour adapter différents signaux cellulaires. Par conséquent, les thérapies ciblant la traduction de l'ARNm représentent une stratégie anticancéreuse prometteuse et de nombreux médicaments ont été développés pour cibler la machinerie d'initiation de la traduction. Un régulateur clé de l'initiation de la traduction est la protéine de liaison à la coiffe de l'ARNm, le facteur d'initiation eucaryote 4E (eIF4E). eIF4E peut être phosphorylé par la kinase 1/2 interagissant avec MAPK (MNK1/2) pour favoriser la tumorigenèse en améliorant la traduction d'un sous-ensemble spécifique d'ARNm qui codent pour des protéines essentielles au développement du cancer. Il a été précédemment démontré par notre laboratoire que la perte de la phosphorylation de eIF4E (p-eIF4E) limite de manière significative les métastases TNBC mais n'affecte pas la croissance tumorale primaire à elle seule. Bien que la monothérapie soit toujours l'approche courante pour traiter le cancer, la thérapie combinée est plus importante car les cellules cancéreuses ont moins de chances de développer une résistance multiple aux médicaments. Ainsi, l'objectif de ce projet est de trouver une nouvelle thérapie combinatoire ciblant à la fois la croissance tumorale primaire du TNBC et les métastases. À cette fin, les partenaires létaux synthétiques de p-eIF4E ont été étudiés en effectuant un criblage génétique impartial à l'aide d'un inhibiteur de MNK1/2 (eFT508) dans une lignée cellulaire TNBC, MDA-MB-231. Grâce à des analyses statistiques et à la validation de cibles à l'aide de petits ARN en épingle à cheveux (shARN) et d'inhibiteurs à petites molécules, nous avons identifié l’inhibition la kinase dépendante de la cycline 4 (CDK4)

par le Palbociclib, un inhibiteur de CDK4/6, qui a montré une forte synergie avec le traitement eFT508. Ces données suggèrent que la thérapie combinée des inhibiteurs de MNK1/2 et CDK4 pourrait être bénéfique pour le traitement simultané des métastases TNBC et de la tumeur primaire, offrant une nouvelle approche thérapeutique dans les thérapies ciblées TNBC.

Acknowledgments

I want to express my deepest appreciation to my supervisor, Dr. Nahum Sonenberg. Through my two and half years of studies in the lab, I have grown tremendously as a young scientist. It has been an honor and an amazing experience to receive mentorship and learn from you.

I would like to extend my sincere thanks to my advisory committee member Dr. Sidong Huang, who has been a supportive mentor. Your expertise in the functional genomics field has helped my project going forward.

Special thanks to my other advisory committee member Dr. Jerry Pelletier, for your valuable advice and assistance with the project.

I also want to thank Dr. Daniella Quail for being my thesis examiner.

There are many current and past lab members whom I am very grateful for. Mehdi Amiri, thank you for guiding me from my first day in the lab. I would not be where I am now without your help and mentorship. Thanks to Jun Luo and Tina Basiri for always being there when I needed help. Special thanks to Zheng Fu from Dr. Huang's lab for giving suggestions and technical assistance for my project. The undergraduate students I supervised, Ellie Zhang and Zilan Li, thank you for helping with many of my experiments. I hope everything you learned from me can truly help you in your future graduate studies.

I gratefully acknowledge the assistance of other lab members, including Dr. Niaz Mahmood, Dr. Peng Wang, Dr. Sunghoon Kim, Dr. Junghyun Choi, Xu Zhang, Sara Bermudez, Shane Wiebe, Gyan Prakash, Trista Lou, Ziying Huang, Reese Ladak, and Michael Bellucci. Thanks to Isabelle Harvey for translating my abstract to French and encouraging me in the lab. Thanks to Eva

Migon, Annamaria Kiss, and Meena Vipparti for all your administrative and technical assistance in the lab.

I also would like to thank the Canderel Graduate Studentship from the Rosalind and Morris Goodman Cancer Institute for the financial support.

Last but not least, I am very grateful for all the life guidance and emotional support from my parents and my significant other, Zhiyang Liu.

Glossary

tRNAs	transfer RNAs
mRNAs	messenger RNAs
eIFs	eukaryotic translation initiation factors
TC	ternary complex
43S PIC	43S pre-initiation complex
$tRNA_i^{Met}$	initiator methionyl tRNA
GTP	guanosine triphosphate
GEF	guanine nucleotide-exchange factor
ISR	integrated stress response
PERK	PKR-like ER kinase
PKR	double-stranded RNA-dependent protein kinase
HRI	heme-regulated eIF2α kinase
GCN2	general control non-derepressible 2
PABP	poly-(A)-binding protein
ATP	adenosine triphosphate
5’ UTR	5’ untranslated region
48S PIC	48S pre-initiation complex
4E-BPs	4E-binding proteins
mTORC1	mechanistic target of rapamycin complex 1
MNK1/2	MAPK (Mitogen-Activated Protein Kinase)-Interacting Kinase ½
MEK	Mitogen-activated protein kinase kinase
ERK	Extracellular signal-regulated kinase

MAPK	mitogen-activated protein kinase
p38	p38 mitogen-activated protein kinases
Ser	serine
Ala	alanine
p-4E	phosphorylated eIF4E
AKT	protein kinase B
RAS	Ras GTPase
PTEN	phosphatase and tensin homolog
PIK3CA	phosphatidylinositol-4,5-bisphosphate 3-kinase catalytic subunit alpha
EGFR	epidermal growth factor receptor
MEFs	mouse embryonic fibroblasts
MET	epithelial-mesenchymal transition
MMP3	matrix metallopeptidase 3
MCL1	MCL1 apoptosis regulator, BCL2 family member
TME	tumor microenvironment
ASOs	antisense oligonucleotides
RAPTOR	regulatory-associated protein of mTOR
asTORi	active-site mTOR inhibitor
mTORC2	mechanistic target of rapamycin complex 1
BCa	breast cancer
ER	estrogen receptor
PR	progesterone receptor
HER2	human epidermal growth factor receptor 2

TNBC	triple-negative breast cancer
PD-L1	programmed death-ligand 1
PARP	poly(ADP-ribose) polymerase
BRCA1/2	Breast cancer type 1/2 susceptibility protein
CDK4/6	cyclin-dependent kinase 4/6
Rb	retinoblastoma protein
E2F	E2 transcription factor
SMARCA4	SWI/SNF related, matrix associated, actin-dependent regulator of chromatin, subfamily A, member 4
RNAi	RNA interference
CRISPR	Clustered Regularly Interspaced Short Palindromic Repeats
CRISPR-KO	CRISPR knockout
CRISPRi	CRISPR interference
hDGG	human druggable genome
shRNA	short hairpin RNA
GFP	green fluorescence protein
MOI	multiplicity of infection
MAGeCK	Model-based Analysis of Genome-wide CRISPR/Cas9 Knockout
Dox	doxycycline
CDK9	cyclin-dependent kinase 9
INTS9	integrator complex subunit 9
CAPN2	calpain 2
ENPEP	glutamyl aminopeptidase

AKR1B1	aldo-keto reductase 1 member B1
UPP1	uridine phosphorylase 1
DMSO	dimethyl sulfoxide
TNNC1	troponin C1
TOP2A	DNA topoisomerase II alpha
CDI	coefficient of drug interaction
PSF	PTB [polypyrimidine tract-binding protein]-associated splicing factor
cPLA2	cytosolic phospholipase A2
dCas9	endonuclease deficient Cas9

Table of Contents

1. Introduction

1.1 mRNA translation overview

In 1958, Francis Crick proposed the concept of the "central dogma of molecular biology," which describes the flow of genetic information in all living organisms, where DNA is the hereditary material that makes RNA, and RNA generates protein to act as the building blocks of the cell[1]. The general information transfer involves DNA replication (DNA copied to DNA), transcription (DNA copied to mRNA), and translation (protein synthesis using mRNA as the template)[2]. Among all, translation of mRNAs is the most energy-consuming process in the cells, which involves tightly controlled interaction of ribosomes, transfer RNAs (tRNAs), messenger RNAs (mRNAs), and other factors to synthesize protein[3,4]. In translation, mRNA is read by the macromolecular machine, the ribosome, to produce amino acid chain[5]. Each amino acid is delivered into the ribosome by specific tRNA that carries a complementary anticodon to the mRNA codon[5]. During this process, the nucleotide sequence of mRNA is thought to be decoded or translated to protein.

mRNA translation can be divided into four stages: initiation, elongation, termination, and ribosome recycling, whereby the initiation stage acts as the rate-limiting step and is governed by various regulatory events[5]. The initiation process begins with the ribosomal subunit and the mRNA being equipped separately with various translation initiation factors (eIFs).

The small (40S) ribosomal subunit, when bound to eIF1, eIF1A, eIF3, eIF5, and the ternary complex (TC), is known as the 43S pre-initiation complex (43S PIC)[5]. The TC is a trimeric protein complex consisting of eIF2 (including α-, β-, and γ-subunits), initiator methionyl tRNA ($tRNA_i^{Met}$), and GTP[6]. TC, especially its eIF2 component, plays a vital role in translation regulation. eIF2B is a multifunctional guanine nucleotide-exchange factor (GEF) that converts

the inactive eIF2-GDP to the active eIF2-GTP state[7]. In addition, eIF2α can be phosphorylated by a group of kinases involved in the integrated stress response (ISR) signaling, such as PKR-like ER kinase (PERK), double-stranded RNA-dependent protein kinase (PKR), heme-regulated eIF2α kinase (HRI), and general control non-derepressible 2 (GCN2)[8]. The phosphorylated eIF2α stabilizes the TC at the GDP-bound state, thereby inhibiting global translation initiation[9].

While the 43S PIC is assembled, the mRNA template is primed with the eIF4F complex. Nuclear-encoded mRNAs harbor a methylated guanosine cap structure at the 5' end (5' cap) and a stretch of adenine bases at the 3' end (poly-A tail) to prevent the exonuclease-mediated mRNA degradation[10]. While the poly-A tail is bound by poly-(A)-binding protein (PABP), the 5' cap is bound by the eIF4F complex, consisting of the cap-binding protein, eIF4E; the scaffolding protein, eIF4G; and the RNA helicase, eIF4A[5]. eIF4G is a large multi-domain protein that binds to the cap-binding eIF4E and serves as a docking site for other proteins involved in the mRNA translation[11]. eIF4A uses ATP to provide RNA helicase activity which can unwind any secondary structures present at the mRNA 5' untranslated region (5'UTR)[6]. With fully equipped 43S PIC and eIF4F-primed mRNA, eIF4G mediates mRNA circularization by binding to the 5' eIF4E and the 3' PABP simultaneously, which leads to the 48S initiation complex assembly[6]. As the 48S PIC recognizes the mRNA start codon through scanning, eIFs are released, and the large (60S) ribosome subunit is recruited to form the translation-competent 80S ribosome[6]. The formation of the complete 80S ribosome marks the end of translation initiation and the beginning of translation elongation[6].

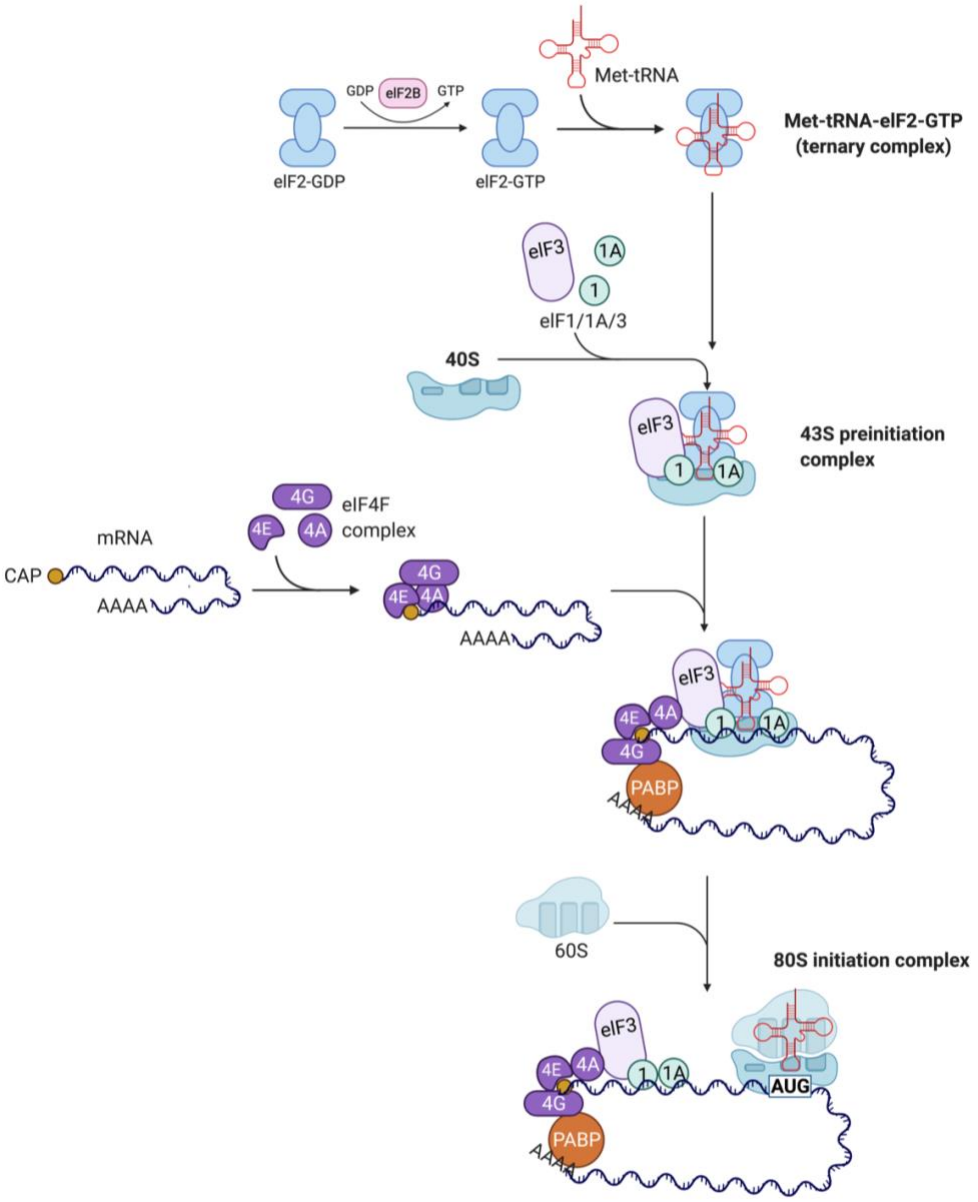

Figure 1. Overview of eukaryotic cap-dependent translation initiation. eIF2 forms the ternary complex (TC) with $tRNA_i^{Met}$ in the presence of GTP; the nucleotide exchange is carried out by the subunit eIF2B. eIF1, 1A, 3, and 5 prime the 40S ribosomal subunit before receiving the TC. The 43S preinitiation complex (PIC) is assembled upon TC joining the 40S subunit. eIF4E forms the eIF4F complex with eIF4G and eIF4A. eIF4E binds to the 5' cap of the mRNA and the scaffold protein eIF4G. The 43S PIC is then loaded to the eIF4F-bound mRNA through eIF3-eIF4G interaction. eIF4G also mediates the mRNA circularization via binding to PABP. The PIC then utilizes the helicase activity of eIF4A to unwind the mRNA secondary structure and scans downstream for the start codon. eIF2-GTP hydrolyzes irreversibly to GDP once the start codon is recognized. With the eIFs being dissociated from the small ribosomal subunit, the 60S ribosomal subunit joins to form the complete 80S ribosome which then begins to synthesize protein. The figure is created with BioRender.com and adapted from Bhat et al., 2015[12].

1.2 eIF4E and its regulation

In 1978, Sonenberg and Shatkin reported a protein with a molecular weight of 24 kDa that can be cross-linked to the 5'cap in mRNA, and this is the discovery of the well-known cap-binding protein, eIF4E[13]. In the next decade, eIF4E was shown to be important in controlling mRNA translation after cloning its cDNA of *Saccharomyces cerevisiae* and human[14,15]. Later, it was found that eIF4E activity is subjected to a tight regulation since it is the limiting factor for translation initiation due to its low expression level compared to other eIFs[16,17].

eIF4E is directly inhibited by the 4E-binding proteins (4E-BPs), which are small translational suppressors that bind eIF4E[5]. Three isoforms of 4E-BPs (4E-BP1, 4E-BP2, and 4E-BP3) have been identified in mammals, which exhibit the same function but have different expression patterns in tissues[16]. By competing with eIF4G, 4E-BPs sequester eIF4E from the active eIF4E pool and mitigates its cap-binding activity[18]. The ability of 4E-BPs to bind eIF4E depends on the phosphorylation state of 4E-BPs[5]. Upon various extracellular and intracellular growth signals, the mechanistic target of rapamycin complex 1 (mTORC1) can phosphorylate 4E-BPs at multiple sites and reduces their affinity to eIF4E, leading to the assembly of eIF4F complex[19-22].

In addition to the mTORC1/4E-BPs axis, eIF4E activity is regulated through phosphorylation on residue Serine 209 by the MAPK (Mitogen-Activated Protein Kinase)-Interacting Kinase 1/2 (MNK1/2)[23]. MNK1/2 are activated by the upstream MEK/ERK and MAPK/p38 pathways in response to mitogenic signals and stress[24-26]. eIF4G, the scaffolding protein in the eIF4F complex, is required to bridge MNK1/2 and eIF4E, allowing subsequent phosphorylation[27]. Interestingly, the phosphorylation of eIF4E is dispensable for viability, as mice with a homozygous Ser209Ala mutation and mice with MNK1/2 double knock-out are viable[28,29]. This implies that eIF4E phosphorylation (p-4E) does not affect global translation. However, the

translation of a subset of mRNAs encoding survival factors was stimulated upon eIF4E phosphorylation[28]. It remains unclear how p-4E can upregulate the translation of specific mRNAs, especially when biophysical studies show that phosphorylation of eIF4E reduces eIF4E-cap interaction[30-33].

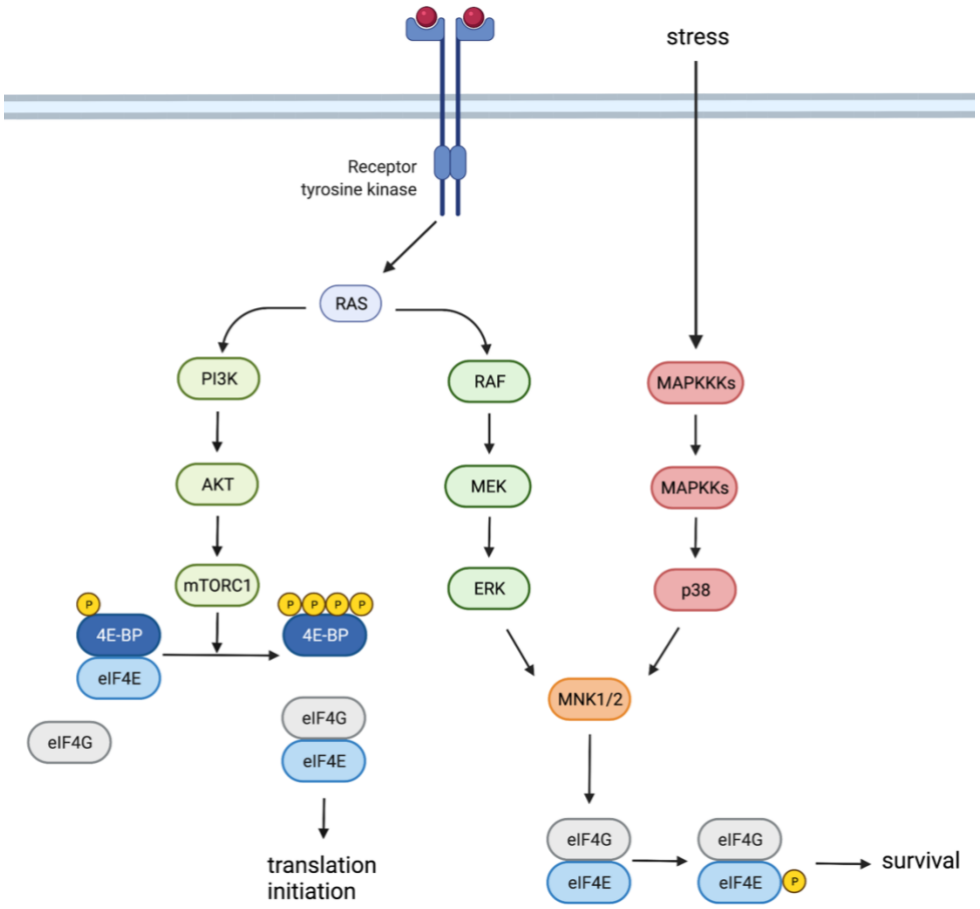

Figure 2. Regulatory pathways of eIF4E activity. 4E-BPs sequester eIF4E availability upon PI3K/AKT/mTORC1 signaling. eIF4E can be activated through phosphorylation at serine 209 by MNK1/2, which receives stimuli from RAF/MEK/ERK and MAPK/p38 pathways. The figure is created with BioRender.com and adapted from Prabhu et al., 2020[34].

1.3 Dysregulated mRNA translation in cancer

Cancer cells are obligated to synthesize protein continuously to sustain their survival, and therefore, mRNA translation is usually aberrantly upregulated[35]. Cancer cells can achieve this

dysregulation via various alterations at the molecular level, such as increasing eIFs expression and enhancing signaling pathways that regulate eIFs activity[35].

The role of deregulated ternary complex formation in cancer cells remains controversial[36]. Some studies showed that the overexpression of eIF2α or its upstream kinases could promote cell transformation in specific contexts[37-39]. Moreover, it has been demonstrated that increased eIF2α phosphorylation allows cancer cells to overcome stress conditions by promoting the translation of stress-response mRNAs[40]. In contrast, other studies showed that a prolonged eIF2α phosphorylation results in cancer cell apoptosis, which inspired numerous research into developing anti-cancer therapies that enhance the phosphorylation of eIF2α[41,42].

eIF4G and eIF4E, however, are classical proto-oncogenes as their overexpression permits cell transformation both *in vitro* and *in vivo*[43-46]. Oncogenic mRNAs encoding MYC, several cyclins, and cyclin-dependent kinases harbor long and highly structured 5'UTRs; thus, their translation heavily relies on the helicase activity of eIF4A and the eIF4F complex formation[47,48]. This subset of mRNAs is referred to as eIF4F-sensitive mRNAs. The expression of all three components of the eIF4F complex is increased in cancer cells, often due to genomic loci amplification or overexpression by the oncogenic transcription factor MYC[12,35,49]. Surprisingly, *c-MYC* mRNA is a translational target of the eIF4F complex, indicating that there is a positive feedback loop exists in cancer cells, where MYC enhances eIF4F expression, and in turn, increases the MYC protein synthesis[50].

Besides eIFs overexpression, mutations in tumor suppressors (for example, *PTEN* loss) and oncogenes (*PIK3CA*, *EGFR*, and *RAS*) often lead to aberrant mRNA translation since these pathways are frequently upstream of eIFs[51]. As the limiting factor in translation initiation, eIF4E availability is tightly restricted by the mTORC1/4E-BPs axis. 4E-BPs act as tumor suppressors

because a non-phosphorylatable 4E-BP1 mutant that always binds to eIF4E can suppress proliferation, whereas losing 4E-BP expression promotes tumorigenesis[52,53]. Therefore, any mutations that result in a hyperactive mTORC1 signaling (e.g., *PTEN* loss, *EGFR* amplification, *PIK3CA* and *RAS* mutation) would lead to hyperactivation of eIF4E; and are commonly found in various cancers[51,54]. In addition to increased eIF4E availability, the oncogenic Ras/Raf/ERK pathway and the upregulated MAPK pathway in cancers lead to hyperactivation of MNK1/2 and thus eIF4E phosphorylation[12]. The phosphorylation of eIF4E also plays a crucial role in tumor progression and metastasis in various types of cancers[55].

1.4 The role of eIF4E phosphorylation in cancer

More than three decades ago, eIF4E was found to act as a proto-oncogene since its overexpression can transform rodent fibroblasts *in vitro*[44]. Twenty years later, it was discovered that overexpression of a non-phosphorylatable eIF4E mutant fails to transform mouse embryonic fibroblasts[28]. Ever since this discovery, investigating the role of eIF4E phosphorylation (p-4E) has always been a major hotspot in cancer research. Increased p-4E expression is a common phenomenon observed in many cancers, including melanoma, breast, colorectal, and prostate cancers[56-59]. Moreover, cancer progression and patient prognosis are associated with elevated p-4E levels[28,60,61]. Identification of p-4E-dependent mRNAs is the key to understanding the mechanisms underlying these observations.

Though no extensive datasets have been published on the mRNAs that rely on p-4E yet, a data set consisting of 35 mRNAs was identified as p-4E-sensitive in mouse embryonic fibroblasts (MEFs)[28]. Using the wild-type and a non-phosphorylatable eIF4E mutant ($eIF4E^{Ser209Ala}$) MEF, polysome profiling results showed that these mRNAs were more actively

translated in the wild-type MEFs[28]. Several factors involved in epithelial-mesenchymal transition (EMT) and angiogenesis, including matrix metalloproteinases, *Mmp3* and *9*, and vascular endothelial growth factor C, *Vegfc*, were among these p-4E-sensitive mRNAs[28]. Later on, a study illustrated that transgenic MMTV-PyMT mice with the eIF4E^{Ser209Ala} mutation develop spontaneous mammary tumors; however, the tumors are resistant to lung metastasis due to impaired p-4E-dependent translation of *Mmp3* and *Snail* mRNAs. Thus, the EMT was mitigated[62]. Besides EMT factors, it was found that p-4E can promote tumorigenesis by upregulating the translation of the anti-apoptotic protein Mcl-1 mRNA in a mouse lymphoma model[55].

Not only does the tumor-intrinsic p-4E level affect the tumorigenesis, but the p-4E status of the tumor microenvironment (TME) also impacts cancer progression. In a mammary tumor model, immunocompetent wild-type mice and mice bearing the whole-body eIF4E^{Ser209Ala} mutation were implanted with wild-type tumor cells. Both mouse strains showed identical primary tumor development, but the eIF4E^{Ser209Ala} mice bearing wild-type tumors were resistant to lung metastasis[63]. This resistance is due to minimal accumulation of the pro-metastatic neutrophils in the lungs of eIF4E^{Ser209Ala} mice[63]. It was found that eIF4E^{Ser209Ala} neutrophils exhibited more apoptosis and their G-CSF-induced survival was significantly impaired compared to the wild-type neutrophils[63]. The survival of these pro-metastatic neutrophils is dependent on p-4E to translate the anti-apoptotic mRNA *Mcl1*[63]. Furthermore, pharmacological inhibition of p-4E in the TME reduced pro-metastatic neutrophil survival and metastatic progression *in vivo*[63].

Notably, p-4E inhibition does not generally affect cell proliferation, as shown by similar rate of proliferation in eIF4E^{Ser209Ala} MEFs compared to wild-type[28]. In addition, several studies using mouse breast cancer models showed that p-4E inhibition (either by chemical compounds or

genetic perturbation) only mitigates lung metastasis but does not reduce primary tumor growth[62-64]. However, p-4E inhibition significantly reduced tumor growth in mouse lymphoma and leukemia models[55,65,66]. These observations imply that p-4E plays a crucial role in cancer progression, but its effect might be different across various cancer types.

1.5 Targeting the eIF4F complex in cancer treatment

As discussed before, translation is commonly upregulated and altered in tumors[4]. Hence, targeting the mRNA translation machinery provides a promising therapeutic avenue in cancer treatment. Since eIF4E is the limiting factor for translation initiation, extensive drug discovery studies focused on inhibiting the eIF4E or eIF4F complex[16,17]. Several approaches targeting the eIF4F complex in cancer can be divided into two categories: the ones targeting eIF4F directly and the ones targeting the upstream regulators of eIF4F[12].

1.5.1 Direct eIF4E inhibitors

eIF4E expression can be directly reduced by antisense oligonucleotides (ASOs), and the cap-binding activity of eIF4E can be inhibited by cap analogues[67,68]. Even though studies have demonstrated prominent anti-cancer effects of these inhibitors without affecting the global protein synthesis, these large molecules' poor permeability and stability remain a challenge for drug delivery *in vivo*[62]. More recently, a pro-drug version of the cap analogue (4Ei-1) with good cell permeability showed an anti-neoplastic effect in lung cancer and breast cancer when converted to its active form upon cellular entry[69]. Alternatively, drugs that disrupt the eIF4E-4G interaction can prevent the assembly of the eIF4F complex, thus inhibiting translation initiation[11]. Small-molecule compounds such as 4EGI, 4E1RCat, and 4E2RCat were identified as inhibitors of the eIF4E-4G interaction from a high-throughput chemical screen[70]. These

molecules mitigate the translation of eIF4F-sensitive mRNAs and have shown promising anti-cancer effects in preclinical models[71].

1.5.2 Direct eIF4A inhibitors

Many eIF4A inhibitors were discovered to suppress translation, all of which exhibited strong anti-cancer effects[34]. A specific category of eIF4A inhibitors allosterically interferes with eIF4A from binding to the mRNA and tempers its helicase activity, including the drug hippuristanol that binds to the C-terminal domain of eIF4A[72]. Pateamine A and silvesterol belong to the other category of eIF4A inhibitors, which induces eIF4A dimerization and increases its RNA-binding affinity in a non-sequence-dependent manner[73]. By accumulating eIF4A stochastically on mRNAs, eIF4A is depleted from the eIF4F assembly[73]. All three eIF4A inhibitors mentioned above show promising efficacy across various *in vitro* and *in vivo* models, where silvesterol has the highest potency, and pateamine A is the most toxic among others due to its covalent inhibition of eIF4A[73-76].

1.5.3 mTOR inhibitors

eIF4E availability can be controlled by the upstream mTORC1/4E-BPs pathway[19-22]. Rapamycin, a natural product from *Streptomyces hygroscopicus*, inhibits mTOR in mammals[77]. Rapamycin and its analogs (rapalogs) allosterically bind to mTOR, which disrupts the interaction between mTOR and the regulatory-associated protein of mTOR (RAPTOR), hence inhibiting only mTORC1 activity[78]. However, rapalogs only exhibit a modest anti-cancer effect due to the incomplete inhibition of the 4E-BPs phosphorylation[79,80]. It was found that rapamycin prevents mTORC1 from phosphorylating selective substrates based on the nature of the residues surrounding substrates' phosphorylation site[81]. For example, S6Ks phosphorylation by mTORC1 can be significantly reduced by rapalogs, whereas; 4E-BPs phosphorylation can only be partially

inhibited[82]. In contrast with rapalogs, the second-generation mTOR inhibitors known as active-site mTOR inhibitors (asTORi) can potently inhibit mTORC1 and mTORC2 since they are ATP competitive inhibitors and block kinase activity directly[83]. This feature potentially allows asTORis to inhibit all mTOR substrates, including a drastic inhibition on 4E-BPs phosphorylation[82,84]. In preclinical cancer models, asTORi showed prominent anti-metastatic and increased potency compared to rapalogs *in vivo*[85]. For instance, AZD2014 is an asTORi with greater and broader antiproliferative effects than rapamycin in multiple breast cancer cell lines and mouse models[83]. Nevertheless, drug resistance is a common complication for mTOR inhibitors. Upon the mTOR signaling halt, cells tend to upregulate other pathways to compensate for the mTOR activity loss[80]. Therefore, cells use alternative routes such as activating MAPK signaling and utilizing the mTORC1-S6K-PI3K feedback loop to increase the pro-survival signal[86,87].

1.5.4 eIF4E phosphorylation inhibitors

eIF4E activity can also be regulated through phosphorylation by the upstream kinases MNK1/2[23]. p-4E has been shown to have important implications in cancer metastasis[62,63]. Several MNK1/2-targeting small-molecule inhibitors have been discovered, such as CGP57380 and cercosporamide[64]. These two compounds reduce the p-4E level and repress malignant cell growth *in vitro*[64]. However, CGP57380 showed no efficacy in decreasing primary tumor growth *in vivo*; but significantly reduced lung metastases[64]. This observation is consistent with other studies where p-4E was diminished using genetic perturbation ($eIF4E^{Ser209Ala}$)[62,63]. The antiproliferative effect observed *in vitro* by CGP57380 and cercosporamide is probably their noteworthy off-target effects[64,88]. To resolve the off-target effects, new MNK1/2 inhibitors have been developed. These include ATP analogs that are competitive inhibitors, protein degraders,

and allosteric inhibitors of MNK1/2[89-91]. Nowadays, the more selective inhibitors are ATP analogs such as SEL201 and eFT508[91,92]. eFT508 (Tomivosertib) is designed by the eFFECTOR company (https://effector.com/) and possesses the lowest off-target effects and the highest affinity against MNK1/2 compared to all other MNK1/2 inhibitors[91]. eFT508 has a half-maximal inhibitory concentration (IC50) of 1 – 2 nM against both MNK1 and 2 in the cell-free assay, compared to an IC50 of 5 – 10 nM for SEL201[91,92]. Currently, eFT508 is in phase II clinical trials in combination with immunotherapy and Paclitaxel chemotherapy to treat blood cancers and solid cancers (NCT02937675, NCT02605083; NCT03258398). Similar to all other MNK1/2 inhibition (either chemical inhibition or genetic perturbation), eFT508 alone is not a potent suppressor of primary tumor growth in many cancer cell lines and *in vivo* models, including unpublished data from the eFFECTOR company[93]. Yet, it has been demonstrated that eFT508 can sensitize rapamycin-resistant colorectal cancer cells to mTORC1 inhibition[94]. Furthermore, several studies on different cancer models also demonstrated the potentiality of inhibiting MNK1/2 in overcoming anti-cancer drug resistance. It was found that p-4E confers resistance to DNA-damaging agents, and cisplatin resistance was overcome by inhibiting MNK1/2 using CGP57380 in breast and cervical cancer cells[95]. Moreover, tamoxifen-resistant ER-positive breast cancer cells were re-sensitized to tamoxifen upon CGP57380 treatment[96]. Therefore, these studies suggested that MNK1/2 inhibition could provide more cancer treatment options when used in combination with other primary therapies.

1.6 Breast cancer and triple-negative breast cancer

Amongst all the cancer types, breast cancer (BCa) is the most common cancer in women worldwide[97]. Patients with breast cancer have different treatment options and prognoses due to

the disease's heterogeneity[97]. To classify BCa subtypes, biological characteristics, such as tumor size, lymph node involvement, histological grade, and molecular markers on the cell surface are widely used[98]. The molecular markers include estrogen receptor (ER), progesterone receptor (PR), and human epidermal growth factor receptor 2 (HER2)[97]. BCa patients with these receptors expressed on the cancer cell surface can be treated by endocrine therapy that targets ER or PR and molecular targeted therapy that utilizes anti-HER2 monoclonal antibody[97].

Besides using hormone receptor status, BCa can also be subtyped based on intrinsic gene signatures, named *luminal-like* and *basal-like*[98]. Around 75% of BCa are ER or PR positive, and these tumor cells express ER, PR, ER responsive genes, and genes usually expressed in luminal epithelial cells[98]. Therefore, this subtype of BCa is called the *luminal-like* group[98]. Within the luminal-like group, the *luminal-A* subgroup represents 50%-60% of all BCa and these tumors have a low histological grade with a good prognosis[98]. On the contrary, the *luminal-B* subgroup is more aggressive as they have a higher histological grade, proliferative index, and worse prognosis[98]. The *basal-like* BCa tends to have an exceptionally high histological grade with lymphocytic infiltration, marking for a high metastasis rate and aggressive clinical behavior[98].

Although considerable progress was made in BCa treatment over the years, a highly aggressive type of BCa, triple-negative breast cancer (TNBC), still lacks available treatment options. TNBC accounts for approximately 15% of all BCa and is defined as a type of BCa that does not express any of the three hormone receptors on the cell surface[97]. Therefore, TNBC is not responsive to traditional targeted BCa therapies[97]. Moreover, gene signature analysis often classifies TNBC as the aggressive subtype, *basal-like* BCa[97]. TNBC patients are often left with the options of surgery and systemic chemoradiotherapy. Still, the efficacy of the treatment is poor as 46% of TNBC patients will develop distant metastasis, eventually leading to cancer

recurrence[97]. Hence, there is still an urgent need to develop new approaches for treating TNBC metastasis.

Recent clinical trials on TNBC utilizing the immune checkpoint inhibitor (Atezolizumab) combined with chemotherapy (Paclitaxel) have shown an improved survival rate[99]. However, the overall survival benefit was only observed in patients with PD-L1 immune cell-positive TNBC[99]. Similarly, PARP inhibitors were FDA-approved as a targeted therapy to treat BCa patients who carry BRCA1/2 mutations[100]. Yet, only 10-20% of all TNBC patients are BRCA mutation carriers[100]. These examples imply that patient-specific medicine may need to be implemented to solve the heterogeneity problem of TNBC.

1.7 Applying the concept of synthetic lethality in developing cancer therapy

The concept of synthetic lethality defines a relationship between two genes, where losing the function of either gene does not affect cell viability, but losing both gene functions concurrently leads to cell lethality[101]. In developing cancer therapies, this principle can be applied in two aspects. The first is to address a cancer-specific mutation (for example, BRCA mutation) with a drug targeting another gene (for example, PARP) which is in a synthetic lethal interaction with the mutation[101]. In such a way, this drug will only be toxic in the cancer cells that harbor this specific mutation[101]. An alternative is to use synthetic lethality to find combination therapies, where each drug targets an entity in the cancer cell and creates synthetic lethality when two drugs are combined [101]. This approach can increase combination therapy efficacy because the effect exerted by two drugs targeting a pair of synthetic lethal partner genes should be far more synergistic than just combining two traditional chemotherapies[101].

Drug resistance is a common problem in cancer therapy as it causes most of the relapses in cancer patients who have initially benefited from successful therapies[102]. The mechanism behind drug resistance is usually cancer cells harnessing alternative pathways to maintain cell growth[102]. Hence, drug resistance could be overcome if the synthetic lethality strategy was utilized to identify the compensatory pathways.

1.7.1 Examples of synthetic lethality

The best-studied synthetic lethal partners are BRCA and PARP[103]. Both genes encode critical factors in DNA repair, where PARP addresses DNA single-stranded break, and BRCA1/2 are responsible for double-stranded break[103]. Individuals who carry a mutation in the BRCA1/2 genes have an increased risk of developing breast and ovarian cancers[103]. By inhibiting its synthetic lethal partner, PARP, the cytotoxic effect only exerts on the tumor that has BRCA1/2 mutation[103].

More recently, a pair of synthetic lethal partners involved in cell-cycle regulation, CDK4/6 and cyclin D1, has been discovered[104]. In proliferating cells, cyclin Ds interacts with CDK4/6, forming a protein complex to phosphorylate retinoblastoma (Rb) in the nucleus[105]. The phosphorylated Rb dissociates from the transcription factor E2F, allowing the released E2F to transcribe the genes necessary for the G1 to S phase transition[105]. In some non-small cell lung cancer and ovarian cancer patients, an essential chromatin remodeling gene, *SMARCA4*, is commonly mutated[104,106]. Due to changes in chromatin accessibility, the locus that harbors the gene encoding cyclin D1 is no longer accessible to transcription factors[93]. Therefore, these patients with *SMARCA4* mutation have a decreased level of cyclin D1, leading to cancer disposition[95]. By using drugs such as Palbociclib that inhibit cyclin D1's synthetic lethal partner, CDK4/6, these patients can have a much better prognosis[104,106].

1.7.2 Discover synthetic lethal interactions using genetic screens

When studying a gene and its associated phenotype, there are two approaches to determining the genetic basis. The forward genetics method begins with a known phenotype and then introduces different mutations to identify the genomic loci responsible for this phenotype[107]. Contrarily, in reverse genetics methods, a known gene of interest is mutated, and then the phenotype is investigated[107]. A genetic screen is an example of reverse genetics, where one introduces various known gene alterations in cells and subsequently examines their resultant phenotypes[108].

In discovering synthetic lethal gene pairs, a reverse genetic screen can be used to identify what gene alteration can lead to a synthetic lethal phenotype[109]. This variant of the genetic screen is known as synthetic lethal screens[109]. These screens are often performed in isogenic cell line pairs where two cancer cell lines are identical but differ in a single gene mutation, such as *TP53* and *KRAS*[110,111]. These cell line pairs are then screened against a functional genomic library to find genetic perturbations that are selectively lethal in the mutated cell line[112]. Alternatively, the screen could be done on a single cell line by dividing the cells into two populations[113]. The gene of interest is inhibited in one of the populations by a small-molecule inhibitor, for example, inhibiting BRAF(V600E) oncoprotein by vemurafenib[113]. Then, both non-treated and treated populations are screened against a library. Thus, the genetic perturbation that selectively created a lethal phenotype in the drug-treated population is identified as the synthetic lethal partner. For instance, EGFR was determined to be the synthetic lethal partner of BRAF in colon cancer[113]. This approach is also known as chemical synthetic lethal screens. A typical *in vitro* chemical synthetic lethal screen consists of the following steps: 1) introduce a genetic perturbation library to a pool of cells; 2) culture cells and treat one of the populations with a drug that targets a gene

of interest; 3) use DNA sequencing and statistical analyses to determine which genetic perturbation resulted in synthetic lethality upon the drug treatment[109].

1.7.3 Different libraries designed for genetic screens

There are many types of functional genomic libraries, such as RNAi and CRISPR knockout (CRISPR-KO) libraries[114]. RNAi such as shRNA is a powerful tool to knock down gene expression, but RNAi screens are prone to off-target effects, limiting its success rate[114]. CRISPR-KO has become a more popular method to edit genetic material due to its lower off-target effect and high efficiency[114]. However, using CRISPR-KO technology in the genetic screen can cause cell anti-proliferation since it introduces double-strand DNA breaks and leads to DNA damage response[115,116]. Alternative versions of CRISPR screens, such as CRISPR-inteference (CRISPRi) screens, have been developed to avoid introducing DNA damage[117]. In addition, the RNAi technique has the benefit of incomplete knockdown phenotypes that differ from the complete knockout phenotypes generated by CRISPR, which is more similar to small-molecule inhibition in cancer therapy[118]. Therefore, synthetic lethal screens using RNAi libraries remain an attractive approach to finding synthetic lethality[118].

1.8 Rationale

Previous studies have demonstrated that targeting phospho-eIF4E (p-eIF4E) by either small-molecule inhibitors or genetic perturbation effectively limits TNBC metastasis but does not affect primary tumor growth in TNBC mouse models[62,63]. Many examples of combination therapy involving MNK1/2 inhibitors have been shown to successfully overcome drug resistance in various cancer types, such as rapamycin, cisplatin, and tamoxifen[94-96]. Hence, MNK1/2 inhibition potentially has many synthetical lethal interactions with other genes. By utilizing the

concept of synthetic lethality and functional genomics screening, we aim to find a novel combination therapy to treat TNBC metastasis and primary tumor simultaneously. To this end, MDA-MB-231, a human TNBC cell line, was selected to perform the *in vitro* synthetic lethal screen. MDA-MB-231 harbors an elevated p-4E level due to its $KRAS^{G13D}$ mutation, leading to hyperactivation of the downstream ERK/MNKs/p-4E pathway[119]. Next, eFT508 treatment was chosen to pharmacologically inhibit MNK1/2-mediated eIF4E phosphorylation in the screen due to its highest potency and selectivity to both MNK1 and 2. Lastly, the human Druggable Genome (hDGG) library, which contains 13,000 doxycycline-inducible shRNAs and targets 2,263 genes, was selected to perform the synthetic lethal screen. The library was chosen because the genes it covers already have available drugs to inhibit them. Therefore, the synthetic lethal targets generated from this screen could directly open up clinical trials for combination therapies in TNBC.

1.9 Hypothesis and aims

Hypothesis: We hypothesize that using the hDGG library and eFT508 to perform a synthetic lethal screen in the MDA-MB-231 cell line would identify multiple synthetic lethal partners of MNK1/2-mediated eIF4E phosphorylation.

Aims:

- Perform pooled synthetic lethal screen using the hDGG library and eFT508
- Use statistical analyses to select a list of potential synthetic lethal candidates
- Validate the candidate list individually to identify authentic synthetic lethal interactions

2. Results

2.1 Utilizing an inducible shRNA library to investigate the synthetic lethal partner of inhibited eIF4E phosphorylation

We set out to use a doxycycline-inducible shRNA library targeting the human druggable genome (hDGG) to identify the synthetic lethal partner(s) of MNK1/2. The hDGG library covers 2263 therapeutically actionable genes, meaning they are susceptible to targeting by drugs. Each gene is targeted by 5 independent shRNAs, and each shRNA contains a unique barcode linked to the shRNA sequence to assist in the later sequencing step. This library was chosen because pharmacological inhibitors targeting the druggable genes identified from our screens would have a higher chance for rapid clinical transition. Additionally, incomplete gene suppression by RNA interference (RNAi) better mimics a drug inhibition[118]. In the LT3GEPIR vector system, GFP and shRNA are both under the inducible T3G promoter (**Fig. 1**). Thus, GFP expression can serve as the direct reporter for shRNA expression.

Figure 1. A simplified schematic of the LT3GEPIR vector system. The puromycin resistance gene and the lentiviral reverse tetracycline-controlled trans-activator 3 (rtTA3) gene are under the phosphoglycerate kinase (PGK) promoter, allowing their constitutive expression. rtTA3 is only active when bound to doxycycline, and the active rtTA3 binds to the inducible T3G promoter to turn on the downstream gene transcription, including *EGFP* and the shRNA. The figure is created with BioRender.com.

2.2 Pre-screen preparation demonstrated the feasibility of the synthetic lethal screen using the hDGG library

Before performing the synthetic lethal screen in MDA-MB-231 cells, several parameters were optimized. Firstly, we investigated the dynamics and stability of eFT508 in MDA-MB-231 cells using Western blotting. It is known that eFT508 potently suppresses eIF4E phosphorylation; and does not impair cell proliferation in solid cancer cell lines, including MDA-MB-231 (unpublished data from eFFECTOR). To determine the optimal eFT508 concentration to use in the hDGG screen, MDA-MB-231 cells were treated with various concentrations of eFT508 in a time course. We found that treating cells with 100 nM eFT508 for 48 or 72 hours showed a profound p-4E reduction, where 10 nM and 20 nM of eFT508 had minimal p-4E suppression after 72 hours (**Fig. 2A**). Moreover, eFT508 was found to be very efficient *in vitro*, which significantly suppressed the p-4E level after only one hour of 100 nM eFT508 treatment (**Fig. 2B**). In addition, the same extent of p-4E reduction was maintained throughout the 72-hour treatment without refreshing the drug-containing media (**Fig. 2B**). This suggests that 100 nM eFT508 can substantially inhibit eIF4E phosphorylation and is stable in cell culture for at least 72 hours. Based on these results, we established the working concentration of eFT508 during the screen to be 100 nM, and determined the timing of media change to be every three days.

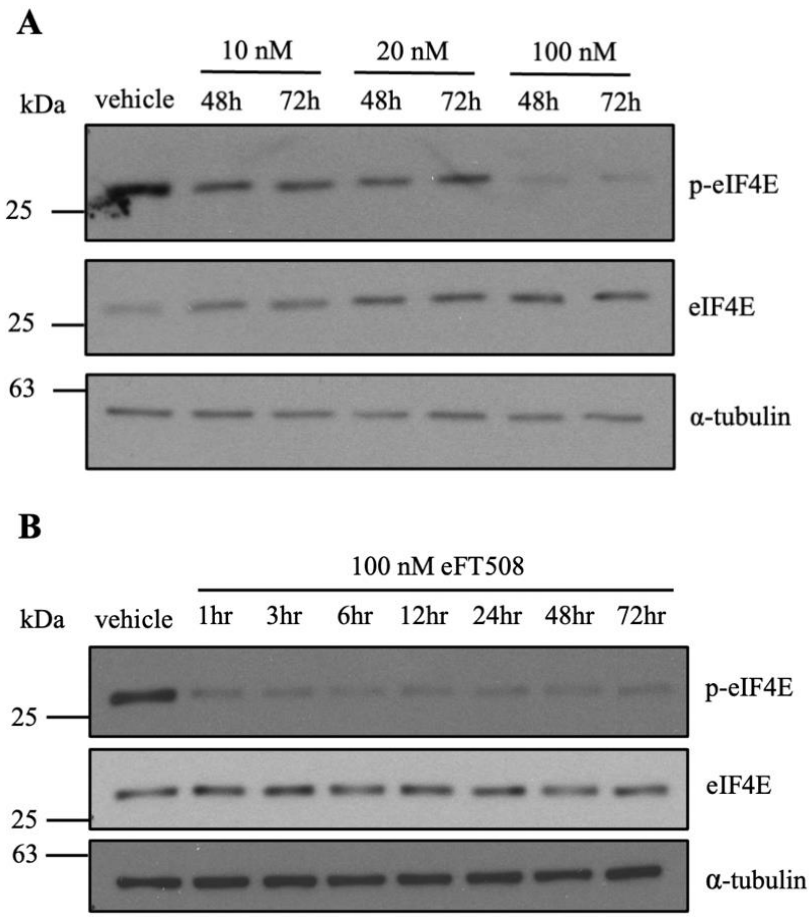

Figure 2. eIF4E phosphorylation in MDA-MB-231 cells is substantially inhibited by eFT508 at 100 nM. A) A Western blot showing the p-eIF4E and total eIF4E levels in MDA-MB-231 cells treated with eFT508 at three different concentrations. The cells were collected 48 and 72 hours after treatment (n = 1). **B)** A Western blot showing the p-eIF4E and total eIF4E levels in MDA-MB-231 cells throughout a 72-hour time course of 100 nM eFT508 treatment (n = 2). The membrane was blotted for total eIF4E first, then stripped and re-probed with the p-4E antibody.

Synthetic lethal screens are essentially negative selection screens, where we observe the drop-out of certain shRNAs as the cells divide. To allow sufficient drop-out, cells are usually cultured for at least 8 doublings in a negative selection screen[120]. We calculated the doubling time of MDA-MB-231 cells by seeding a known number of cells and re-counting them a few days later. Using Roth's computational method, the doubling time for MDA-MB-231 cells was

determined as 31.82 hours (Roth V, 2006 http://www.doubling-time.com/compute.php). Therefore, 8 doublings would translate into 254.56 hours, equivalent to 11 days in culture.

The key to linking a synthetic lethal phenotype to its corresponding genetic perturbation is ensuring each cell receives only one genetic modification[120]. During transduction, single virion uptake by each cell is done through transducing cells at a very low multiplicity of infection (for example, MOI < 0.5)[120]. Hence, we performed pilot transduction to determine the viral titer of the lentiviral hDGG library that Dr. Sidong Huang (Department of Biochemistry, McGill University) provided. MDA-MB-231 cells were transduced with different volumes of the lentivirus and selected using puromycin. An MOI of 0.3 was determined as a 25-30% survival rate after puromycin selection (see **Methods 4.3.2**).

Furthermore, this cell population transduced at MOI 0.3 was tested for doxycycline (dox) induction to validate the shRNA expression under the T3G promoter. We found that starting from 200 ng/mL of doxycycline, more than 90% of the transduced cells were GFP-positive after 18 hours of induction **(Fig. 3)**. Moreover, the GFP-positive cell population increased by less than 5% when the doxycycline concentration increased from 200 to 1000 ng/mL **(Fig. 3)**. To minimize the cell toxicity caused by doxycycline, the lowest concentration possible, 200 ng/mL, was chosen to induce GFP and shRNA expression during the actual screen.

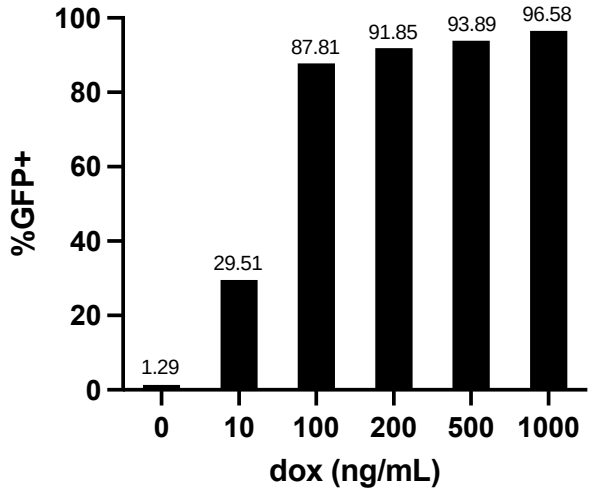

Figure 3. The expression of the reporter GFP was induced by doxycycline in transduced MDA-MB-231 cells. MDA-MB-231 cells transduced at MOI 0.3 were induced with doxycycline at different concentrations for 18 hours. The GFP-positive population was quantified using flow cytometry (n = 1).

2.3 hDGG screen identified many potential synthetic lethal partners of MNK1/2

Using the hDGG library, we performed a pooled genetic screen to determine genes whose inhibition is synthetically lethal to reduced eIF4E phosphorylation in the MDA-MB-231 cell line. MDA-MB-231 cells were infected with the lentiviral hDGG library at an MOI of 0.3 to ensure single virion uptake in each cell. Following the transduction, cells were selected using puromycin and cultured in the presence of doxycycline and eFT508 or vehicle for eight doublings (11 days). Cells without doxycycline-induction were used as a control to measure the initial shRNA abundance after transduction and to rule out straight lethal genes. To achieve a good library representation, a 1000-fold coverage of the library size (13,000 shRNAs) was maintained constantly by keeping at least 1.3×10^7 cells in each population[120]. At the endpoint of the screen, genomic DNA from each cell population was extracted to PCR-amplify the barcodes linked to the inserted shRNAs. The relative abundance of the shRNA constructs within each cell population was determined by next-generation sequencing on the Illumina sequencing platform.

Over 96% of the shRNA sequences were retained in all populations, showing sufficient library coverage for the screen. **(Fig. 4)**.

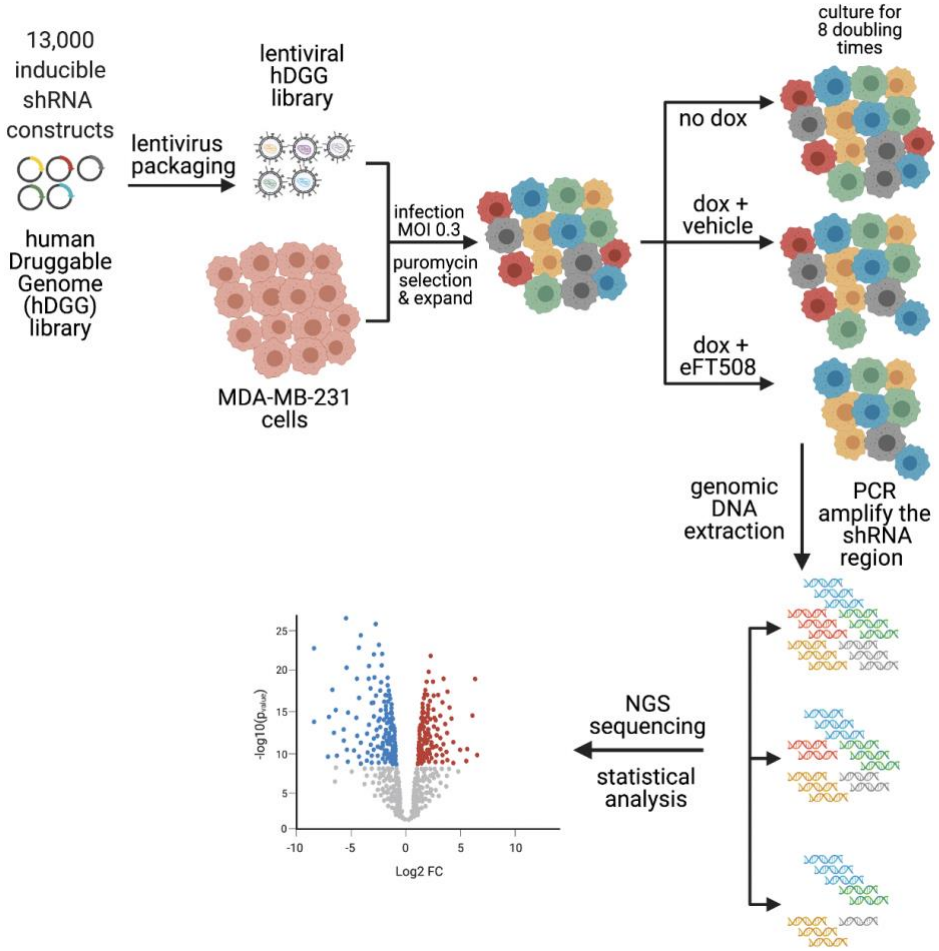

Figure 4. A schematic outline of the shRNA screen for identifying synthetically lethal partners of MNK1/2. MDA-MB-231 cells were infected with the lentiviral hDGG library at an MOI of 0.3. Puromycin-selected cells were divided into three populations with different treatments as indicated. All three populations were cultured for eight doublings (11 days) to allow sufficient drop-out. Genomic DNA was extracted from each population after 11 days and the inserted shRNA within the genome was PCR-amplified. The relative abundance of shRNAs in the hDGG library was analyzed by next-generation sequencing, and synthetic lethal candidates were selected using MAGeCK software analysis.

After the screen was completed, we used MAGeCK statistical software package to analyze the sequencing data[121]. We set up an arbitrary cutoff line for shRNA constructs that had been sequenced at least 200 times and depleted at least 30% in the treated population to mitigate sequencing noise **(Fig. 5A)**. It was observed that a population of shRNAs significantly dropped-out upon eFT508 treatment **(Fig. 5A)**. Essential genes were first removed from generating the candidate list by comparing the uninduced population (no dox) with the induced population (dox+vehicle). From the MAGeCK analysis, 47 genes were depleted by more than 30% (log_2 fold change < -0.5) in the eFT508 treatment group with p-values < 0.05 **(Fig. 5B)**.

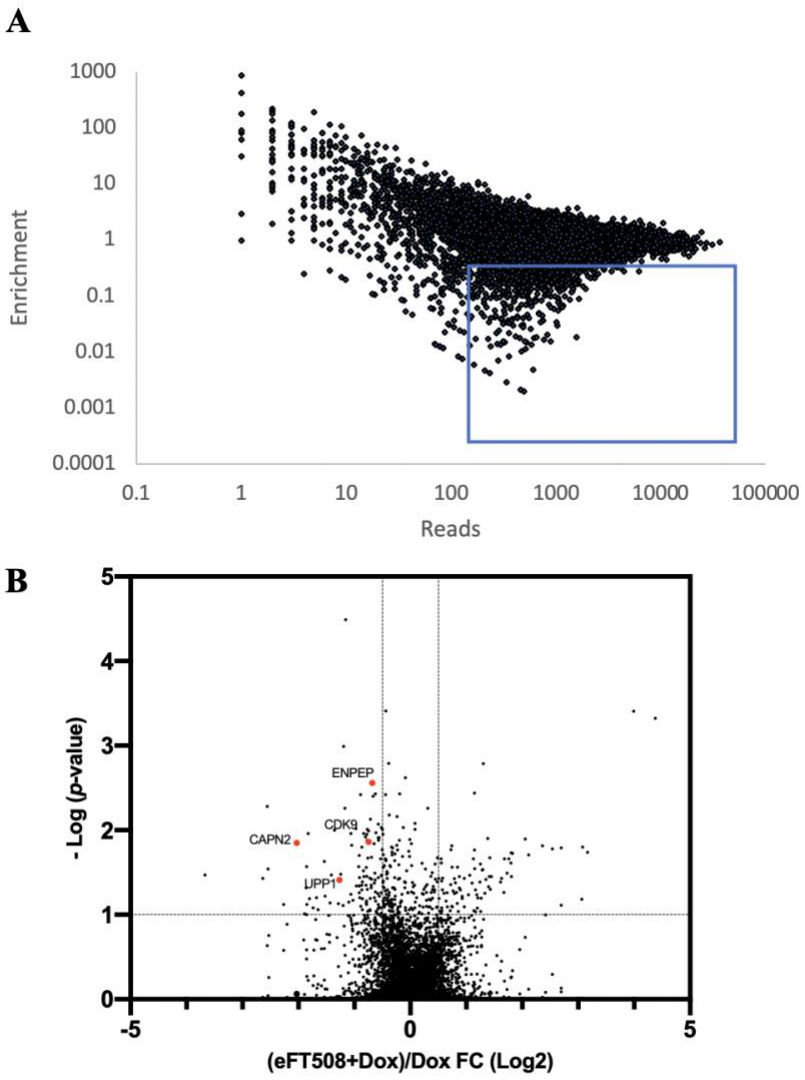

Figure 5. hDGG screen identified many potential synthetic lethal partners of MNK1/2 inhibition. A) The relative abundance of the shRNAs from the hDGG screen. The x-axis shows the number of reads in the untreated population and the y-axis shows the enrichment (the reads ratio of eFT508 treated/untreated). The arbitrary cutoff line (reads > 200, fold change < -0.5) for significantly dropped out shRNAs is indicated by the blue box. **B)** A volcano plot representing the significant genes (enriched, unchanged, and dropped out) in the eFT508 treatment group compared to the vehicle control group. The x- and y-axis represent the Log_2 fold change and the -Log p-value, respectively. The data was analyzed by MAGeCK, and several top synthetic lethal candidates were indicated in red.

Based on the performance of each independent shRNA, 13 genes were chosen as top candidates for synthetic lethal partners **(Table I)**. Among the top targets are genes controlling transcription, such as cyclin-dependent kinase 9 (CDK9) and integrator complex subunit 9 (INTS9)[122]; genes involved in cell adhesion such as calpain 2 (CAPN2)[123]; genes related to tumorigenesis such as glutamyl aminopeptidase (ENPEP)[124]; and genes regulating metabolism such as aldo-keto reductase 1 member B1 (AKR1B1)[125]. We also compared the list of our top targets with the list of mRNAs that are translationally regulated by p-eIF4E in MEFs[28], revealing only one gene which encodes for uridine phosphorylase 1 (UPP1) in the pyrimidine salvage pathway[126].

Table I. Top genes that are potentially synthetic lethal to MNK1/2 inhibition

Gene	**Log_2 fold change**	**p-value**
INTS9	-3.66	0.038
AKR1B1	-2.73	0.071
CTSC	-2.58	0.059
GALK1	-2.46	0.071
PRIM1	-2.06	0.061
CAPN2	-2.05	0.027
UPP1	-1.67	0.024
IFNA8	-1.32	0.018
DRD2	-1.23	0.013
CDK9	-0.76	0.055
MAPK6	-0.67	0.013
ENPEP	-0.67	0.006
IRAK2	-0.53	0.002

2.4 Multiple synthetic lethal candidates from MAGeCK analysis could not be validated

After narrowing the candidates to 13 genes from the hDGG screen, we individually validated their synthetic lethality with MNK1/2 inhibition using individual shRNA knockdown. We used at least two shRNAs targeting each gene to minimize off-target effects. The shRNAs are from the Mission TRC library and constructed in a non-inducible pLKO vector. The shRNA bacterial prep was provided by the Genetic Perturbation Service (GPS) of Goodman Cancer Research Institute and Biochemistry at McGill University. MDA-MB-231 cells stably expressing these shRNAs were generated through lentiviral transduction. Each stably knockdown cell line was then subjected to a colony formation assay to evaluate its synthetic lethality to MNK1/2 inhibition. Colony formation assay is a type of *in vitro* cell survival assay based on the property of a cell growing into a colony after a period of time[127]. A small number of cells from each knockdown cell line was seeded in the presence of DMSO or eFT508, and was cultured for 11 days to allow colony formation. Colonies were fixed with paraformaldehyde and stained using crystal violet.

The 13 top hits were divided into halves for validation to reduce parallel workload. We first validated 7 genes from the candidate list using two shRNAs per gene. However, these knockdown cell lines showed no inhibition of proliferation when treated with eFT508 compared to the DMSO control group (**Supplementary Fig. S1**). This data suggested that the first half of the candidate list could not be validated as true synthetic lethal partners of MNK1/2, assuming the shRNAs used in this experiment generated sufficient knockdown. To resolve this concern, the shRNA knockdown efficiencies were tested for the second half of the list before proceeding to the validation assay. To test the knockdown efficiencies of the stable cell lines, qRT-PCR or Western blot were used to assess the mRNA and protein levels, respectively (**Fig. 6A, B**). The

knockdown efficiencies of CAPN2 and CDK9 shRNAs were tested using Western blot because no suitable qPCR primers could be found due to multiple splice variants. Amongst the 13 tested shRNAs, only shCTSC#1 and shCDK9#1 did not generate sufficient knockdown. Next, these stable cell lines with known knockdown efficiencies proceeded to colony formation assays. We first observed that cells with different knocked-down genes showed various antiproliferative effects compared to the non-targeting control shRNA (shCTRL) (**Fig. 6C**). Nevertheless, similar to the first half candidates, all validated knockdown cell lines showed no difference in proliferation when treated with eFT508 **(Fig. 6C)**. These results implied that the top synthetic lethal candidates from the hDGG screen using MAGeCK analysis could not be validated using individual shRNA knockdown.

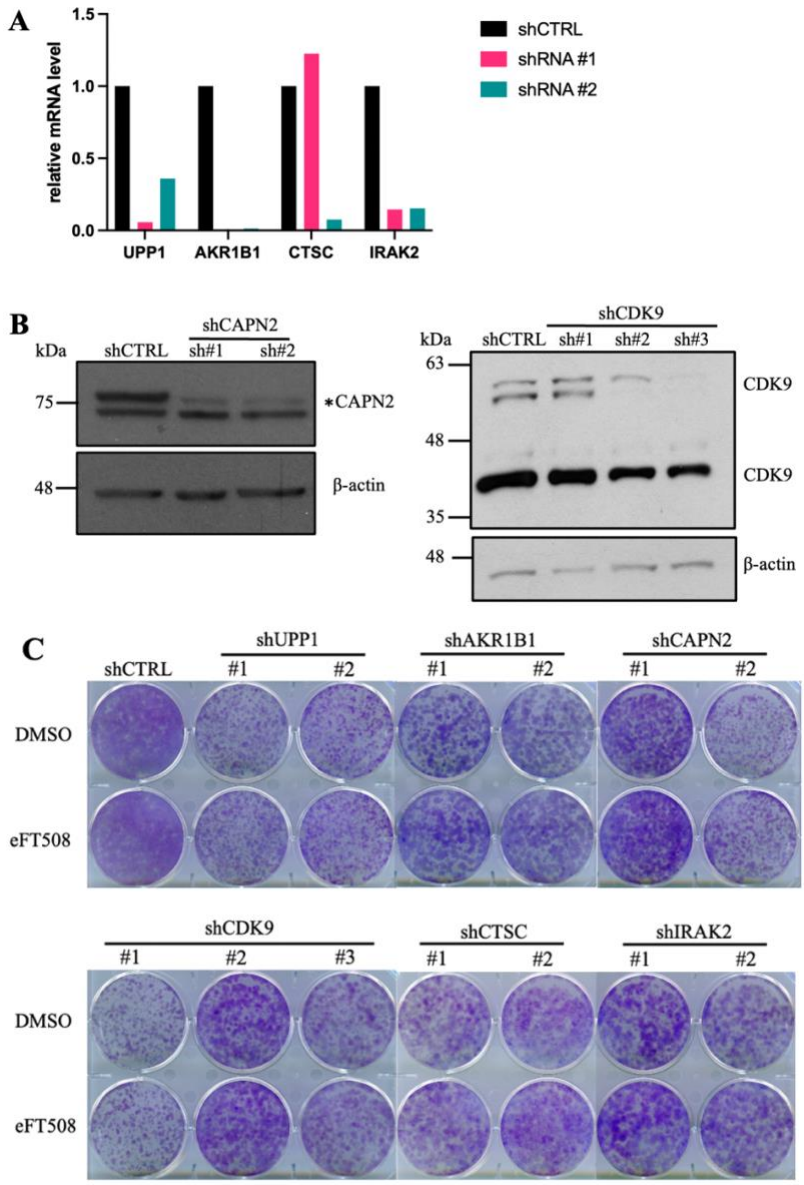

Figure 6. MDA-MB-231 cells with various candidate genes knocked down showed no synergistic antiproliferation with eFT508 treatment. A) Relative mRNA level of UPP1, AKR1B1, CTSC, and IRAK2 in corresponding knockdown cell lines, normalized to shCTRL. The experiment was done in technical triplicates. **B)** Western blots illustrating the CAPN2 and CDK9 protein levels in corresponding knockdown cell lines (n = 1). The shRNAs targeting CAPN2 only showed significant knockdown on the major isoform at 80 kDa, indicated by the asterisk. The shRNAs #2 and #3 targeting CDK9 showed significant knockdown on all three isoforms (one at 42 kDa and two around 55 kDa), while shRNA #1 did not generate pronounced knockdown. **C)** Colony formation assays for different knockdown cell lines of MDA-MB-231. 5000 cells were seeded in each well of 6-well plates and cultured in the presence or absence of 1 μM eFT508 for 11 days. For visualization, colonies were fixed using paraformaldehyde and stained with crystal violet (n = 2).

2.5 Pharmacological CDK4 inhibition shows a strong synergistic effect with MNK1/2 inhibition *in vitro*

Since the top 13 candidate genes generated by MAGeCK analysis did not yield true synthetic lethal partners of MNK1/2 inhibition, we re-analyzed the synthetic lethal screen data manually. First, we used the same cutoff line as before to select the shRNAs that selectively dropped out in the eFT508 treatment group (reads > 200, fold change < -0.5, p-value < 0.05). Next, we looked for genes that had multiple shRNAs that significantly dropped out. In the new analysis, we identified two shRNAs targeting a gene not previously identified among the initial MAGeCK candidates. This new gene encodes for cyclin-dependent kinase 4 (CDK4), which is a well-known cell cycle regulator[105]. The two CDK4 shRNAs showed significant negative fold changes and low p-values in the eFT508 treatment group **(Fig. 7A)**. However, MAGeCK ranks a gene based on the overall performance of all five shRNAs, and CDK4 was not a top hit here because only 2 out of 5 shRNAs were significantly dropped out (**Fig. 7B**). Since the inducible shRNAs in the hDGG library were induced at the dox concentration of 200 ng/mL, there is a possibility that the other three shRNAs targeting CDK4 could not generate sufficient knockdown at this dox concentration. Thus, CDK4 could be a false negative which was missed in the MAGeCK analysis. Several other genes were also identified in the new analysis and could be classified as potential false negatives for further validation, such as troponin C1 (TNNC1) and DNA topoisomerase II alpha (TOP2A).

A

shRNA ID	Gene	Log_2 fold change	p-value
hDGG_00575	CDK4	-3.75	0.0022
hDGG_00574	CDK4	-2.31	0.0052
hDGG_00572	CDK4	0.60	0.98
hDGG_00573	CDK4	-0.45	0.13
hDGG_00571	CDK4	0.41	0.85

B

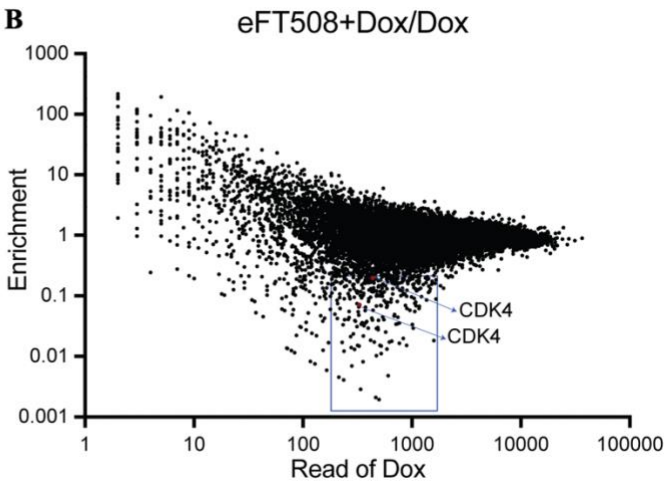

Figure 7. CDK4 is potentially a synthetic lethal candidate for MNK1/2 but is not identified in the MAGeCK analysis. A) A table showing the performance of all five shRNAs targeting CDK4. The two shRNAs that dropped out upon eFT508 treatment are highlighted in red. **B)** A dot plot illustrating the relative abundance of the shRNAs from the hDGG screen. The x-axis shows the number of reads in the untreated population and the y-axis shows the enrichment (the reads ratio of eFT508 treated/untreated). The blue box indicates the arbitrary cutoff line for significant shRNAs (reads > 200, fold change < -0.5). Blue arrows and red dots indicate the two shRNAs targeting CDK4 that showed drop-out.

From previous validations of the MAGeCK-generated top hits, we noticed that using pLKO-based shRNAs could not replicate the synthetic lethal phenomenon observed in the hDGG screen. These pLKO-based shRNAs are not inducible, therefore, the cells subjected to validation assays were already expressing the shRNAs for some time before the actual eFT508 treatment. On the contrary, the cells in the hDGG screen expressed inducible shRNAs. Thus, their shRNA expression and MNK1/2 inhibition by the eFT508 treatment happened concurrently. Therefore, to better mimic the conditions in the actual screen, we utilized a small-molecule inhibitor that targets CDK4, along with eFT508 to treat MDA-MB-231 cells simultaneously during the validation assay. There are no inhibitors that can selectively inhibit CDK4 due to its high similarity to CDK6; hence we utilized Palbociclib, a potent CDK4/6 inhibitor, to validate the potential synthetic lethal interaction between CDK4 and MNK1/2. Firstly, we performed a

Western blot to confirm the activity of Palbociclib and eFT508 in MDA-MB-231 cells. Cells were treated with two different concentrations of Palbociclib, and the Rb phosphorylation (p-Rb) status was evaluated in their protein lysate since it is a downstream substrate of CDK4. We observed that p-Rb and p-eIF4E significantly decreased upon Palbociclib and eFT508 treatment, respectively (**Fig. 8**). Notably, the total Rb level was also reduced, and p-4E was surprisingly increased when cells were treated with Palbociclib, which will be discussed later. Together, eFT508 and Palbociclib were effective in terms of inhibiting the phosphorylation of their downstream substrates in MDA-MB-231 cells.

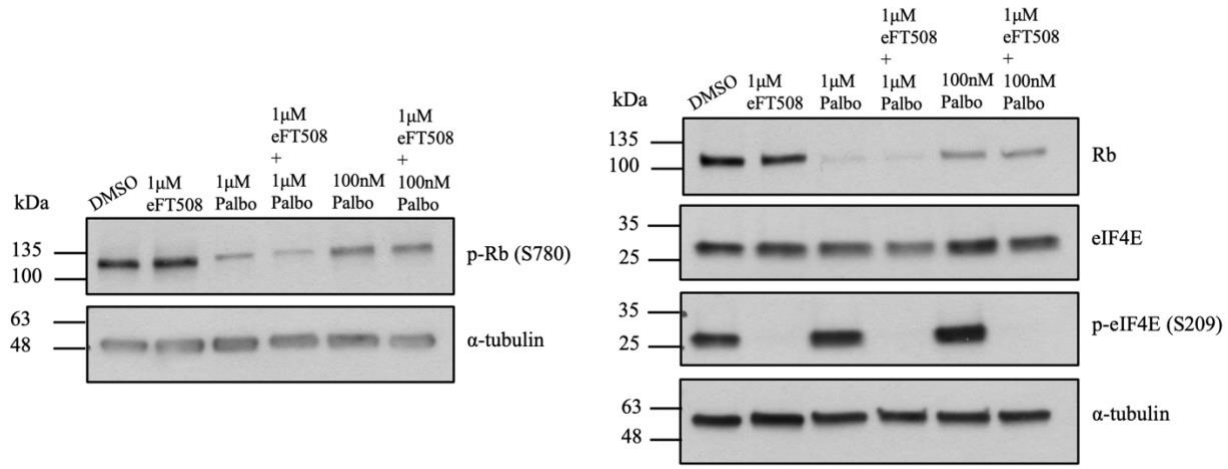

Figure 8. Palbociclib and eFT508 are effective in inhibiting Rb and eIF4E phosphorylation. Western blots showing the levels of total/p-Rb and total/p-4E in MDA-MB-231 cells treated with different concentrations of Palbociclib and eFT508 for 18 hours. The total Rb antibody could not be stripped off completely, therefore, total Rb and p-Rb were blotted on different membranes using the same protein lysate to avoid signal cross-contamination (n =3).

In cell-free assays, Palbociclib has an IC_{50} around 10 nM in inhibiting CDK4/6[128]. To assess the cytotoxicity of short-term Palbociclib treatment on MDA-MB-231 cells, we tested a range of Palbociclib concentrations using a CellTiter-Glo viability assay. This assay determines the number of viable cells based on the quantitation of the ATP present. We observed that treating MDA-MB-231 cells with different concentrations of eFT508 for 72 hours did not affect

cell viability until the concentration reached as high as 30 μM (**Fig. 9A**). Moreover, the cell viability decreased moderately upon Palbociclib treatment, where viability reduced to 64.5% when Palbociclib concentration was at 3 μM (**Fig. 9A**). Interestingly, an additional 10% reduction in viability was observed when cells were treated with both Palbociclib and eFT508 (**Fig. 9A**). Consistent with this, a cell proliferation assay using a real-time imaging system illustrated that the antiproliferative effect of Palbociclib was enhanced by approximately 10% by combining with eFT508 treatment (**Fig. 9B**). These results suggested that eFT508 has a synergistic effect with Palbociclib on suppressing MDA-MB-231 cell growth.

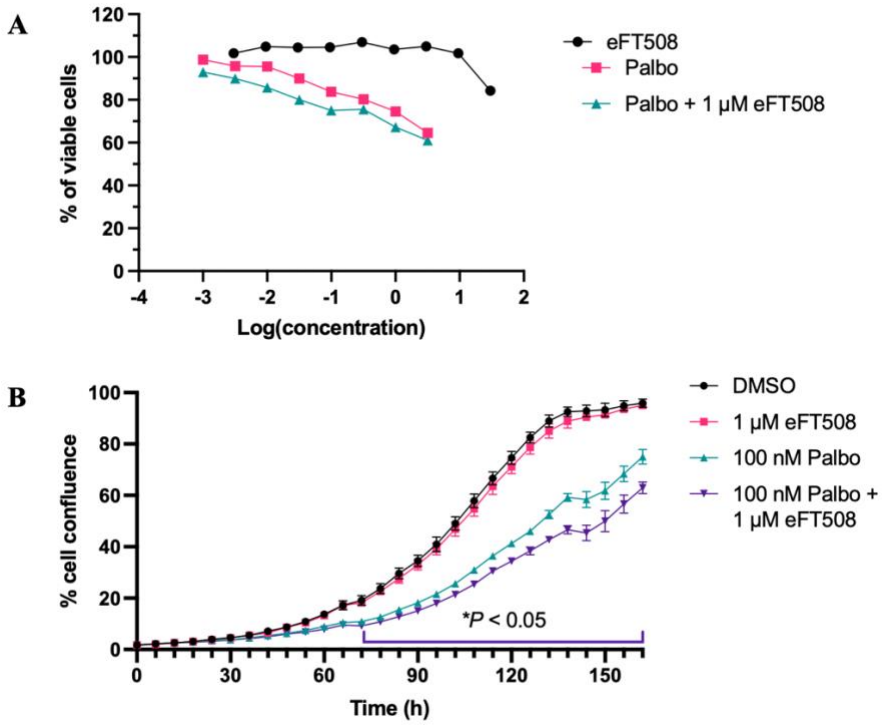

Figure 9. MNK1/2 inhibition has an additive effect with MNK1/2 inhibition on repressing cell proliferation *in vitro*. A) Cell viability assay of MDA-MB-231 cells treated with various concentrations of Palbociclib with or without 1 μM eFT508. The drug treatment lasted 72 hours before cells were lysed to measure the ATP level through fluorescence reading, reflecting the viable cell counts. The x- and y-axes represent the log values of concentrations used and viable cell percentage, respectively (n = 1). **B)** Real-time cell proliferation assay of MDA-MB-231 cells treated with vehicle, eFT508 and/or Palbociclib for 7 days. Images of the cells were taken every 6 hours using IncuCyte FLR, and cell proliferation was visualized based on the cell confluence in the images. The graph showing significant slower proliferation upon eFT508-Palbociclib treatment compared to Palbociclib alone has a $P < 0.05$ for every time point from hour 72-162; by parametric multiple unpaired t-tests. Error bars: mean ± SD of three technical replicates (n = 1).

In keeping with our above findings that the eFT508 treatment has an additive effect on reducing cell proliferation with CDK4/6 inhibition, we found that long-term eFT508-palbociclib combination treatment can substantially impair the colony-forming ability of MDA-MB-231 cells (**Fig. 10A**). Furthermore, we used ImageJ to quantify the stained intensities of the colony formation assay. The quantification showed around 30% synergy when cells were treated with

the eFT508-palbociclib combination compared to Palbociclib mono-treatment starting at 50nM of Palbociclib (**Fig. 10B**). Next, we calculated the coefficient of drug interaction (CDI) to classify the nature of the interaction between eFT508 and Palbociclib as synergistic, additive, or antagonistic[129,130]. Using the following equation: $CDI = AB/(A \times B)$[124], the calculated CDI values showed that the eFT508-palbociclib combination at indicated doses is strongly synergistic in suppressing MDA-MB-231 cell proliferation (**Fig. 10C**). Taken together, these findings suggest that pharmacological CDK4 inhibition shows a strong synergistic effect with MNK1/2 inhibition in MDA-MB-231 cells.

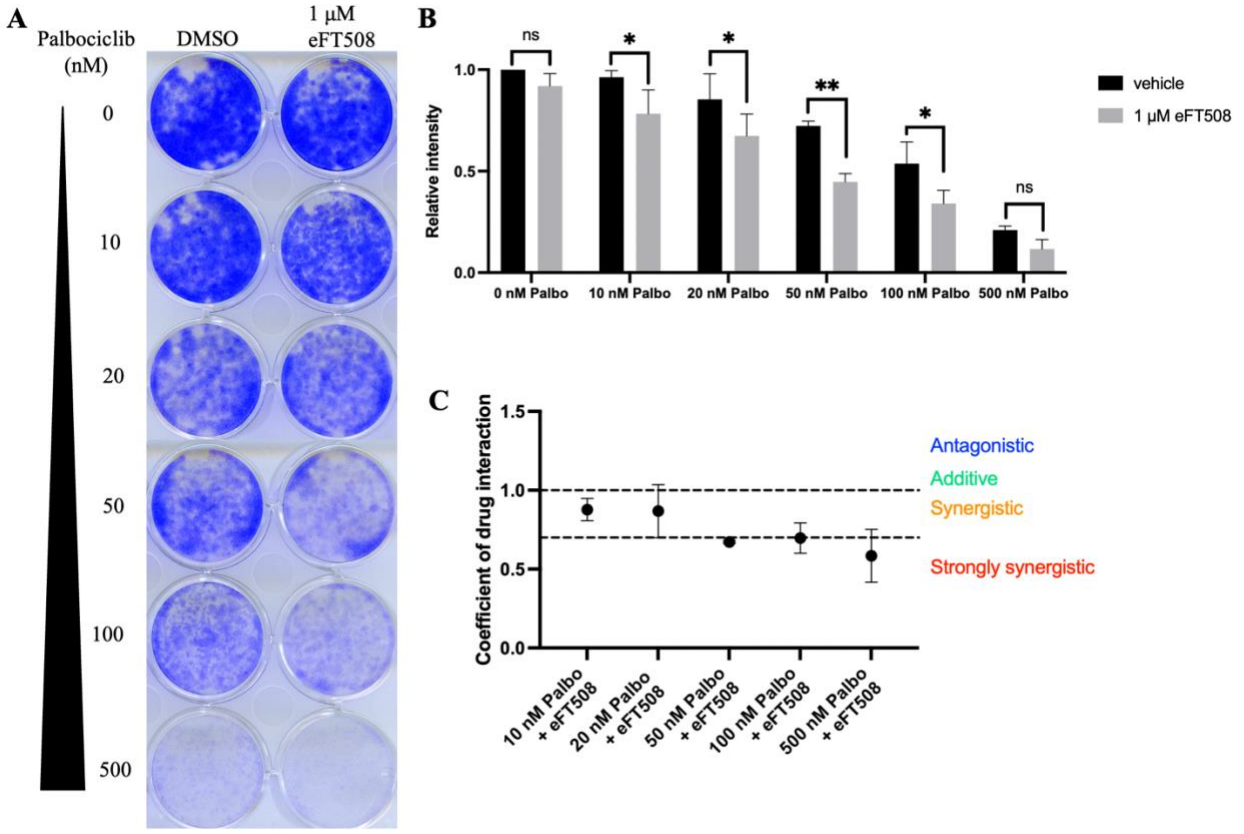

Figure 10. CDK4/6 inhibition is strongly synergistic with MNK1/2 inhibition in suppressing colony formation *in vitro*. A) Colony formation assay illustrating MDA-MB-231 cell growth. Cells were seeded at a density of 5000 cells/well in a 12-well plate, and were treated with different concentrations of Palbociclib with or without eFT508 for 8 days. For visualization, colonies were fixed using paraformaldehyde and stained with crystal violet. **B)** A bar graph showing the relative staining intensity of each well. The stained plates were scanned and quantified using the ImageJ ColonyArea plugin. *, $P < 0.0332$; **, $P < 0.0021$; by two-way ANOVA with multiple comparisons using the Bonferroni test; (n = 3). **C)** The coefficient of drug interaction (CDI) of the Palbociclib-eFT508 combination in MDA-MB-231 cells. CDI > 1.0 indicates antagonistic effect; CDI = 1.0 indicates additive effect; CDI between 0.7 and 1.0 indicates synergy; and CDI < 0.7 indicates strong synergy. Error bars represent mean ± SD (n = 3).

3. Discussion

In this project, we utilized a potent MNK1/2 small-molecule inhibitor, eFT508, and a genetic screen to leverage the synthetic lethal partner(s) of inhibited eIF4E phosphorylation in triple-negative breast cancer. From this synthetic lethal screen, we uncovered that pharmacological CDK4 inhibition by Palbociclib synergizes with p-4E reduction by eFT508 to suppress MDA-MB-231 TNBC cell line growth *in vitro*.

3.1 Palbociclib-eFT508 combination shows synergy but not synthetic lethality

Based on the colony formation assay done in long-term Palbociclib-eFT508 treatment, we characterized this drug combination as strongly synergistic, in which the Palbociclib-eFT508 group had a 30% lower viability compared to the Palbociclib-only group. Nonetheless, according to the screen sequencing data, the two inducible shRNAs targeting CDK4 in the library showed an 80-90% decrease (i.e., Log_2 fold changes of -2.31 and -3.75) when comparing the eFT508-dox population to the dox-only population. This indicated that the synergy of Palbociclib-eFT508 treatment does not recapitulate the synthetic lethality we observed in the screen. This discrepancy can be partly explained by the nature of the Palbociclib drug. The coefficient of drug interaction (CDI = AB/A×B) can be used to characterize drug-drug interactions, where A and B represent the effect of individual drugs and AB the combinatorial treatment effect, measured by colony formation assay. In the context of computing Palbociclib-eFT508 interactions, "AB" represents the viability of cells treated with the eFT508-Palbociclib combination relative to the DMSO control, and "A" or "B" corresponds to the viability of cells treated with only one of the drugs compared to the DMSO control. This yields CDI = 0.46/(0.71×0.96) = 0.67 for 50 nM Palbociclib and 1 μM eFT508. Based on the CDI readout, drug interactions can be divided into various types of effects: antagonistic effect, or CDI>1.0, (2) additive effect, or CDI=1.0, (3)

synergy with CDI between 0.7 and 1.0, and (4) strong synergy with CDI < 0.7[129,130]. In order to get a small CDI representing the synthetic lethal phenotype, treatment with individual drugs must minimally affect cell viability. However, Palbociclib itself is already toxic to the cells and can significantly reduce cell viability (A = 0.71). It is known that Palbociclib is a small-molecule inhibitor that binds to the ATP pockets of both CDK4 and CDK6 to inhibit their activity[128]. Since CDK4/6 both function as suppressors of cell cycle progression, Palbociclib showed significant clinical toxicity[128], and illustrated considerable *in vitro* toxicity in MDA-MB-231 cells at concentrations as low as 50 nM (**Fig. 9**). On the contrary, only CDK4 was inhibited in our hDGG shRNA screen setting, which most likely gave rise to reduced toxicity levels compared to CDK4/6 dual inhibition by Palbociclib. Thus, individual doxycycline-induced shRNAs targeting CDK4 may reconcile the varied outcomes observed from the screen and subsequent validations.

3.2 Possible mechanisms underlying the CDK4-MNK1/2 synergistic genetic interaction

The relationship or interaction between two genes, such as synergistic effects and synthetic lethal effects, can now be systematically studied in cancer cell lines using high-throughput genetic screens[131]. Despite this progress, only a handful of genetic interactions have been reported as synthetic lethal, and even fewer synthetic lethal interactions could be reproduced across different models in multiple studies[131]. This major barrier in synthetic lethality studies is known as low penetrance[132]. A computational study by Dr. Christopher Lord uncovered that robust genetic interactions usually involve gene pairs whose protein products were in a protein complex[131]. For instance, cyclin D1 and CDK4 form a protein complex that

regulates the cell cycle, and this pair has been identified as being potently synthetic lethal in several cancer cell lines[104,106].

In the case of CDK4 and MNK1/2, no known evidence has suggested that they are involved in a protein complex. Notwithstanding, MNK1/2-mediated downstream eIF4E phosphorylation promotes the translation of cyclin D1 mRNA[95]. Therefore, the synergistic effect observed in the CDK4-MNK1/2 pair might be an alternative representation of CDK4/6-cyclin D1 synthetic lethal interaction. Since p-4E is upstream of cyclin D1 translation, targeting the p-4E would generate a less robust genetic interaction with CDK4, leading to a synergistic effect instead of a synthetic lethal one, as we observed in the hDGG screen validation. In keeping with the theory, the Western blot, showing the effectiveness of Palbociclib and eFT508, illustrated an increase in p-4E level when cells were treated with Palbociclib (**Fig. 7**). This observation is consistent with the literature, where increased phosphorylation of eIF4E is commonly observed in different cancer cells after being exposed to stress stimuli, including chemotherapeutic treatments, such as gemcitabine, paclitaxel, cisplatin, and doxorubicin[133,134]. Mechanistically, these stress stimuli can trigger ERK and MAPK signaling to increase the p-4E level for cellular survival. Upon Palbociclib treatment, MDA-MB-231 cells may utilize the increased p-4E level to help translate more cyclins, particularly cyclin D1. It has been observed that cyclin D1 was upregulated in Palbociclib-resistant cancer cells which were subjected to prolonged Palbociclib treatment[104,135]. As such, cells may compensate for CDK4 activity loss by increasing cyclin D1 level via p-4E-dependent translational upregulation. In cells treated with the Palbociclib-eFT508 combination, their p-4E level is substantially reduced, and the compensatory mechanism would thus be suppressed. Therefore, the p-4E-mediated cyclin D1 compensation would not occur in cells treated with the Palbociclib-eFT508 combination, explaining the synergy observed in our

results. In the future, the protein level of cyclin D1 can be evaluated in Palbociclib-eFT508-treated cells to support our theory.

Another possible mechanism underlying the Palbociclib-eFT508 synergy involves the phosphorylation of 4E-BP1 by CDK4. Recently, a research group discovered that 4E-BP1 is a CDK4 substrate via *in vitro* kinase assays[136]. By treating cancer cells such as MDA-MB-231 with Palbociclib and Rapamycin *in vitro*, the researchers illustrated that Palbociclib further inhibited 4E-BP phosphorylation and is independent of mTORC1 inhibition[136]. The synergy between Palbociclib and eFT508 could be explained by double eIF4E inhibition through reduced phosphorylation by eFT508 and enhanced 4E-BP1 binding by Palbociclib. This eIF4E double inhibition may lead to repressed mRNA translation of certain survival factors known as p-4E targets, such as MCL1, c-MYC, and cyclin D1.

For future work, the protein and mRNA levels of cyclin D1 and phosphorylated 4E-BP1 can be assessed in the cells treated by the Palbociclib-eFT508 combination to further investigate the underlying mechanism. Polysome profiling can also be performed to identify the translational upregulation of the previously mentioned p-4E-sensitive mRNA species.

Apart from all, the reduced p-4E level was thought to be the sole readout of MNK1/2 inhibition by eFT508. Nevertheless, MNK1/2 have other substrates besides eIF4E, such as hnRNPA1, Sprouty2, PTB [polypyrimidine tract-binding protein]-associated splicing factor (PSF), and cytosolic phospholipase A2 (cPLA2)[137]. Although the phosphorylation of these substrates has not yet been validated *in vivo* and their contribution to tumorigenesis remains unknown[138], we cannot rule out the possibility that the eFT508-Palbociclib synergy can act through this p-4E-independent mechanism. Thus, it is important to establish an eIF4E Ser209Ala

knock-in MDA-MB-231 cell line and further validate the synthetic lethal targets using this approach.

3.3 hDGG screen quality

Our hDGG synthetic lethal screen successfully identified a synergistic genetic interaction between CDK4 and MNK1/2 in reducing TNBC cancer cell growth *in vitro*. However, the interaction was not robust enough to be classified as synthetic lethality. Moreover, the top targets from this screen had a low validation rate (1 out of 14 targets), which raises the question of whether an unsuitable validation scheme was implemented using pLKO-based non-inducible shRNAs. During the validation process where shRNA is constitutively expressed, target knockdown occurs shortly after the lentiviral transduction[139], leading to a non-synchronization between the gene knockdown and MNK1/2 inhibition by the eFT508 treatment. Hence, we propose to re-validate the top targets using the doxycycline-inducible shRNA system or small-molecule inhibitors since all targets are druggable by definition.

Although the validation methods might have been erroneous, and as such, we did not observe any synthetic lethality, the low validation rate still poses some questions about the screen quality overall. The first quality control of a synthetic lethal screen is to look for essential gene drop-out. If the inducible shRNA knockdown system functioned during the screen, known essential genes should be dropped out in the dox-only population. Therefore, we mined data from the Dependency Map (DepMap) to find the identified essential genes in the MDA-MB-231 cell line. Out of 19 top essential genes from DepMap, the hDGG library covered 3 of them, and they all showed significant drop-out upon doxycycline addition ($\log_2$ fold change around -2). Likewise, other known essential genes, such as eIF4E and mTOR, also showed significant drop-

out. Based on this quality control, we conclude that the doxycycline-inducible shRNA library was functional during the screen.

Lastly, a limited gene coverage of the hDGG library may also explain the lack of synthetic lethal interactions. Although the library has already encompassed 2757 therapeutic genes, using a larger library might identify more reliable synthetic lethal targets. A genome-wide library can be utilized for future works to expand the gene coverage. We propose to perform a genome-wide screen using the latest CRISPR technology due to its much smaller off-target effects than shRNAs[114]. Several genome-wide CRISPR knockout (CRISPR-KO) libraries against the human genome have illustrated immense feasibility in numerous publications, such as GeCKO developed by the Zhang lab, TKO designed by the Moffat lab, and Brunello by the Doench lab[140-142]. Nonetheless, the CRISPR-Cas9 KO approach might raise concerns due to double-strand DNA break-mediated cell anti-proliferation[143]. This anti-proliferation is independent of the actual physiological essentiality of the targeted gene, but rather due to the nature of Cas9-mediated DNA double-stranded break[143]. The anti-proliferation effect will present as random gene drop-out in the screen, resulting in a significant false-positive rate[143]. CRISPR interference (CRISPRi), a better-tolerated version of CRISPR-Cas9, uses a nuclease-deactivated Cas9 (dCas9) tethered to an inhibitory transcription factor domain to down-regulate gene expression; and thus allows for transient gene down-regulation and without introducing DNA damage response. Recently, a CRISPRi library (Dolcetto library) developed by the Doench lab has shown prominent gene dropout, and outperformed existing CRISPRi libraries. Therefore, using a genome-wide CRISPR-KO or CRISPRi library to repeat the synthetic lethal screen might reveal more targets in the future.

3.4 Significance

In conclusion, this project demonstrated a successful *in vitro* synthetic lethal screen using an shRNA library despite a low validation rate, which could be improved by adopting better validation methods. Our data suggest a strong synergistic effect between CDK4 and phosphor-eIF4E inhibition in reducing TNBC cell growth *in vitro*, thus, providing a sound rationale for a potential clinical trial using the available MNK1/2 inhibitor to enhance the performance of CDK4/6 inhibitors in treating triple-negative breast cancer.

Since TNBC is a heterogeneous disease, different cell lines likely have varying synthetic lethal partners for p-4E inhibition. Although we identified the Palbociclib-eFT508 synergy in the MDA-MB-231 cell line, it does not necessarily mean that this synergy would apply to other TNBC cell lines. Therefore, performing the same hDGG screen in various TNBC cell lines can identify not only universal synthetic lethal targets to all TNBC; but also specific synthetic lethal targets in different TNBC cell lines. The identified universal synthetic lethal targets can shed light on generating broad-spectrum combination therapy (with eFT508) for all TNBC patients. Alternatively, personalized combination therapies with eFT508 can be designed according to the different mutation profiles that each TNBC patient has.

4. Materials and Methods

4.1 Cell culture and shRNA lentiviral transduction

The MDA-MB-231 cell line was a generous gift from Dr. Lynne-Marie Postovit (Queen's University, Kingston, Canada), and HEK293T cell line was purchased from ATCC. MDA-MB-231 was cultured in RPMI medium supplemented with 10% fetal bovine serum (FBS), and 1% penicillin/streptomycin. HEK293T was cultured in DMEM medium with 10% FBS and 1% penicillin/streptomycin. All cell lines were tested for Mycoplasma contamination routinely via a PCR-based method. All cell lines were maintained at 37 °C and 5% CO_2 for fewer than 20 passages. Lentiviral particles were generated using Lipofectamine 2000 (ThermoFisher Scientific) as the transfection reagent and as per the protocol described at https://www.addgene.org/protocols/plko/#E. MDA-MB-231 cells were transduced for 8 hours and subsequently selected in 2 μg/mL puromycin for 48 hours. Transduced cells were immediately collected for further experiments.

4.2 Compounds and antibodies

Tomivosertib (eFT508) was provided by eFFECTOR Therapeutics, Inc. (Solana Beach, CA, USA), and Palbociclib (S1116) was purchased from Selleck Chemicals (Houston, TX, USA). The antibodies used for Western blot are shown below in **Table II**.

Table II. Antibodies for Western Blotting

Targeted Protein	Company	Catalog number
eIF4E	BD Biosciences	610270
p-eIF4E (S209)	Abcam	76256
Rb	Cell Signaling Technology	9313S
p-Rb (S780)	Cell Signaling Technology	9307
α-Tubulin	Santa Cruz Biotechnology	sc-23948
β-actin	Sigma-Aldrich	A5441
CDK9	Cell Signalling Technology	C12F7
CAPN2	GeneTex	102499

4.3 Pooled synthetic lethal shRNA screen

shRNAs that target human druggable genes (hDGG library) are in the lentiviral LTEGEPIR (pRRL) vector, where the GFP reporter and shRNA construct are under the doxycycline-inducible T3G promoter, and puromycin resistance gene is under the PGK promoter acting as the mammalian selection marker. Lentiviral supernatant was provided by Dr. Sidong Huang (McGill University, Montreal, Canada) as a generous gift.

4.3.1 Screen preparation

Before determining the viral titer, a range of 0 – 8 μg/mL of polybrene concentrations was tested on MDA-MB-231 cells for toxicity. Puromycin titration (0 - 3 μg/mL) was also performed beforehand to determine the optimal concentration and treating time for puromycin selection. The doubling time of MDA-MB-231 cells was determined by seeding 7×10^5 cells in a 15-cm tissue culturing dish, then recount the number of cells after 72 hours. The mathematical calculation was done through the computational method derived by Roth. V (Roth V. 2006 Doubling Time Computing, http://www.doubling-time.com/compute.php).

4.3.2 Viral titer determination

To determine the viral titer for transductions, MDA-MB-231 cells were seeded in a 6-well plate (7×10^5 cell/well). Cells were incubated overnight to allow attachment. The attached cells were then transduced on the next day in the presence of polybrene (6 μg/mL) and virus at various volumes (0, 10, 25, 50, 100, and 200 μL virus). Eight hours after transduction, virus-containing media was refreshed with regular cell culture media. Transduced cells were then recovered overnight before proceeding to puromycin selection. The next day, transduced cells from each well were transferred into two 6-cm plates where one of the plates is cultured in the presence of 2 μg/mL puromycin. After 48 hours, all 12 plates were counted for viability. A survival rate of

30% compared to the non-selected populations corresponds to a multiplicity of infection of 0.3, and is used for later library screening.

4.3.3 Doxycycline induction test

A doxycycline induction test was performed in the transduced cells with the MOI 0.3. The transduced cells were plated in a 6-well plate at a 7×10^5 cell/well density, and incubated overnight to allow cell attachment. Regular media was replaced with the doxycycline-containing media at various concentrations (0 – 1000 ng/mL), and cells were induced for 18 hours. The next day, induced cells were detached from each well, and 200 μL of each cell suspension was added to a 96-well plate. The frequency of GFP-positive cells under each doxycycline concentration is analyzed by a flow cytometer (Guava®easyCyte™). The lowest doxycycline concentration that gave rise to more than 90% of GFP expression was used for inducing later library shRNA expression.

4.3.4 synthetic lethal screen

The actual transduction for the screening was done in 15-cm plates, with a scaling factor of 10 to the 6-well plates for viral titer determination. MDA-MB-231 cells were transduced by the lentivirus pool (MOI 0.3) and selected using 2μg/mL puromycin. Cells were then pooled and plated at 3.25×10^6 cells per 15-cm plate for three different conditions (no doxycycline control, 200 ng/mL doxycycline + 0.1% DMSO, and 200 ng/mL doxycycline + 100 nM eFT508). Each condition contains four 15-cm plates, giving rise to a 1000-fold coverage of the hDGG library. The medium was refreshed every two days, and cells were sub-cultured into new 15-cm plates every four days (maintaining the 1000-fold coverage). After 12 days of cell culture, genomic DNA was isolated from 1×10^7 cells per condition using the High Pure PCR Template Preparation kit [141].

shRNA inserts were extracted from 48 μg genomic DNA per condition by PCR amplification. The PCR amplification was done in two steps (PCR1 and PCR2) using the following cycling conditions: 98 °C, 30 s; (2) 98 °C, 10 s; [99] 60 °C, 20 s; (4) 72 °C, 60 s; (5) to step (2), 16 cycles; (6) 72 °C, 5 min; (7) 4 °C. Indexes and adaptors for deep sequencing (Illumina) were added into PCR primers. 10 μL of PCR1 product was used as a PCR2 template for each condition. The final PCR2 products were purified using NucleoSpin Gel and PCR Clean-up kit (Takara Bio) according to the manufacturer's manual. Subsequently, the purified PCR2 products were run on an 8% TBE-polyacrylamide gel to perform gel extraction as described in Ingolia's paper[144]. The statistical analysis of the screen was processed using MAGeCK statistical software package (version 0.5.4)[121].

The primers used are shown below in **Table III**:

Table III. Primer sequence for amplifying shRNA inserts within the genomic DNA

Condition	Forward primer	Reverse primer
PCR1_no dox	CCCTACACGACGCTCTTCCGATCTCGTGATTAGTGAAGCCACAGATGT	CAAGCAGAAGACGGCATACGAGATCATGCTCCAGACTGCCTTGG
PCR1_dox	CCCTACACGACGCTCTTCCGATCTACATCGTAGTGAAGCCACAGATGT	
PCR1_dox +eFT508	CCCTACACGACGCTCTTCCGATCTGATCTGTAGTGAAGCCACAGATGT	
PCR2_all conditions	AATGATACGGCGACCACCGAGATCTACACTCTTTCCCTACACGACGCTCTTCCGATCT	CAAGCAGAAGACGGCATACGAGAT

4.4 RNA isolation and RT-qPCR

Cultured cells were collected and subjected to RNA extraction using 800 μL of TRIzol (Invitrogen). The fractions were then mixed by vigorous shaking and incubated at room temperature for 5 min. 200 μL of chloroform was added to each extract, followed by vigorous shaking for 2 min at room temperature. The extracts were then centrifuged at 12,000 rpm for 15 min at 4 °C. The upper aqueous layer was transferred to a pre-chilled tube containing 90 μL of

sodium acetate (3 M, pH 5.5). 500 µL of isopropanol was added to the aqueous extract and was mixed immediately by inverting the tube. The RNA extract in isopropanol was then stored at -80 °C overnight to improve RNA yield. The frozen RNA solution was centrifuged at 20,000 rcf for 35 min at 4 °C. The precipitated RNA pellet was then washed with ice-cold ethanol (80%) and left to dry at room temperature. The dried pellet was dissolved in RNase-free water, and the concentration was measured by Nanodrop Spectrophotometer (ThermoFisher Scientific) and adjusted to a final concentration of 250 ng/µL.

cDNA synthesis was performed using a SuperScript III Reverse-Transcriptase Kit (Invitrogen) and Oligo-dT (Invitrogen) according to the manufacturer's instructions. Quantitative PCR was performed using SYBR Green (Invitrogen) and CFX Connect Real-Time PCR Detection System (Bio-Rad) equipment. The primers that were used are shown in **Table IV**. All samples were done in triplicates, and each reaction contained 50 ng of cDNA and 4 fmol of each primer.

Table IV. Primer sequence for qPCR validating shRNA knockdown efficiency

Gene	Forward primer	Reverse primer
UPP1	TCACAATGATTGCCCCGTCA	TGCCCATACCATGACTGACA
AKR1B1	CGTCTCCTGCTCAACAACGG	TACGTGCACCACAGCTTGC
CTSC	ACTGCTCGGTTATGGGACCAC	TAAGTGGTCACCTTGCTGCC
IRAK2	AGAAGCTCAGAGAGACAGCCT	GACCATGCAGGTACTCGACG

4.5 SDS-PAGE and Western blots

Cells were lysed with RIPA buffer (50 mM Tris pH 7.4, 1% NP40, 0.1% SDS, 150 mM NaCl, 2 mM EDTA pH 8) supplemented with protease and phosphatase inhibitors. The lysate was incubated at 4 °C with rotation for 30 min, and was centrifuged at 15,000 rpm for 15 min at 4 °C. The supernatant was collected and used for SDS-PAGE followed by Western blot.

Proteins were denatured by adding 5× loading buffer (250 mM Tris-HCl, pH 6.8; 8 % w/v SDS; 0.2 % w/v bromophenol blue; 40 % v/v glycerol; 20 % v/v β-mercaptoethanol) and subjected to SDS-PAGE followed by transferring onto nitrocellulose membrane. Membranes were blocked in 5% skim milk solution (in 0.1 % TBST) and subjected to primary antibody incubation.

4.6 Plasmids

pLKO shCTRL vector was purchased from Sigma-Aldrich (SHC002). Individual pLKO shRNA plasmids were from the Mission TRC library (Sigma) provided by Genetic Perturbation Service (GPS) of Goodman Cancer Research Institute and Biochemistry at McGill University: shUPP1#1 (TRCN0000161305), shUPP1#2 (TRCN0000165386); shAKR1B1#1 (TRCN0000046411), shAKR1B1#2 (TRCN0000288741); shIRAK2#1 (TRCN0000196789), shIRAK2#2 (TRCN0000000549); shCAPN2#1 (TRCN0000003540), shCAPN2#2 (TRCN0000272781); shCDK9#1 (TRCN0000000494), shCDK9#2 (TRCN0000199892), shCDK9#3 (TRCN0000000498); shCTSC#1 (TRCN0000003608), shCTSC#2 (TRCN0000003609); shCDK4#1 (TRCN0000000362), shCDK4#2 (TRCN0000196986); and shCDK6#1 (TRCN0000010081), shCDK6#2 (TRCN0000009878).

4.7 Cell viability assay

Cultured cells were seeded into 96-well plates (seeding number depends on the cell size and proliferation rate). After 24 hours, serial dilutions of drugs were added to cells to final concentrations of 0.001 to 100 μM. Cells were then incubated for 72 hours, and cell viability was assessed using the CellTiter-Glo viability assay (Promega). The relative survival rate in the presence of drugs was normalized to the untreated control.

4.8 Colony formation assay and coefficient of drug interaction calculation

Cells were seeded into 6-well or 12-well plates and cultured in the absence or presence of corresponding drugs for 8 – 12 days (seeding number and culturing time depend on the cell size and proliferation rate). The drug-containing medium was refreshed every two days. At the endpoint of the colony-formation assay, cells were fixed with 4% paraformaldehyde in PBS and subsequently stained with crystal violet (0.5% w/v). Stained and dried plates were scanned at high resolution for ImageJ quantification using the ColonyArea plugin. The ColonyArea plugin quantifies the stained colonies based on the colony size as well as its intensity, which can reflect the cell density difference[145]. The CDI value for each Palbociclib concentration was calculated using the equation: $CDI = AB/(A \times B)$[130]. "AB" was the relative staining intensity of the eFT508-Palbociclib combination compared to the DMSO control; "A" or "B" was the relative staining intensity of the groups treated with only one of the drugs compared to the DMSO control.

4.9 Incucyte cell proliferation assay

Cultured MDA-MB-231 cells were seeded into 6-well plates at a density of 3×10^4 cells per well. Cells were incubated overnight to allow attachment before the drug treatment. Images of the cells were taken using the phase-contrast setting every 6 hours using Incucyte FLR (Essen Bioscience, Michigan, US). The drug-containing medium was refreshed every three days. Cell proliferation was analyzed based on the cell confluence in the images.

4.10 Statistical analysis

Statistical significance of biological replicates of colony formation assays was carried out by two-way ANOVA with multiple comparisons using the Bonferroni test, where *, $P < 0.0332$; **, $P < 0.0021$; ***, $P < 0.0002$; ****, $P < 0.0001$. Cell proliferation data collected using the IncuCyte FLR was evaluated with parametric, multiple unpaired *t*-tests on each time point. Unadjusted P-values < 0.05 were considered statistically significant. GraphPad Prism 9 software was used to generate graphs and statistical analyses.

5. Supplementary data

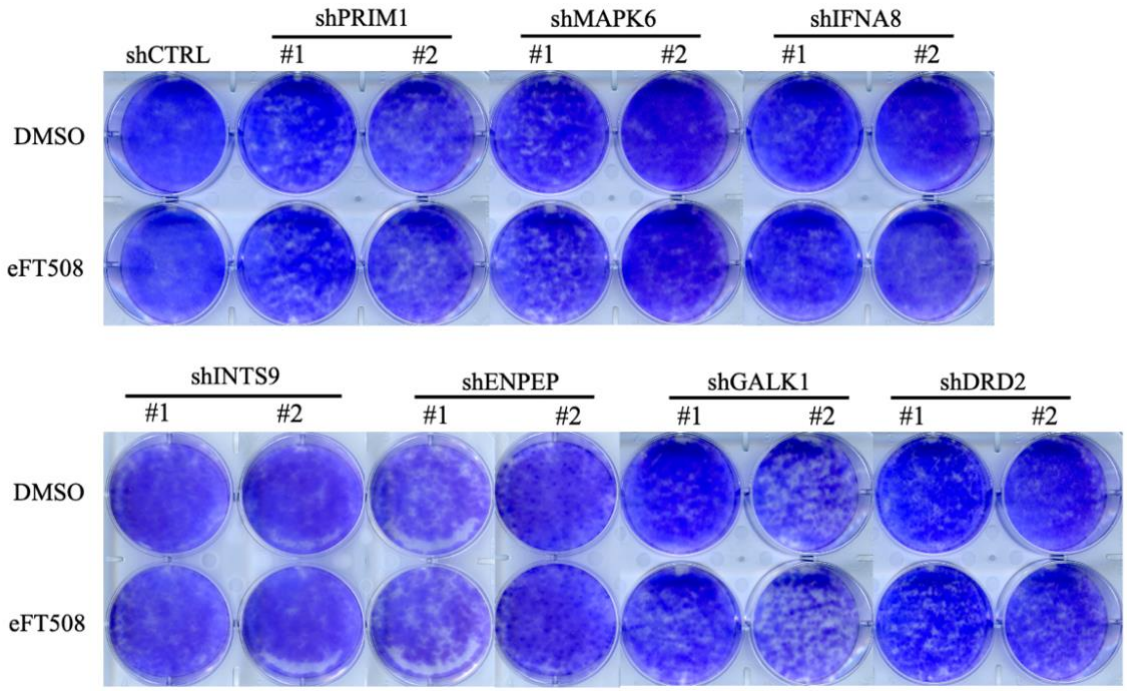

Figure S1. MDA-MB-231 cells with various candidate genes knocked down showed no synergistic antiproliferation with eFT508 treatment. Colony formation assays for different knockdown cell lines of MDA-MB-231. 5000 cells were seeded in each well of 6-well plates and cultured in the presence or absence of 1 μM eFT508 for 11 days. For visualization, colonies were fixed using paraformaldehyde and stained with crystal violet.

6. References

1 Crick, F. H. On protein synthesis. *Symp Soc Exp Biol* **12**, 138-163 (1958).

2 Ille, A. M., Lamont, H. & Mathews, M. B. The Central Dogma revisited: Insights from protein synthesis, CRISPR, and beyond. *Wiley Interdiscip Rev RNA*, e1718, doi:10.1002/wrna.1718 (2022).

3 Buttgereit, F. & Brand, M. D. A hierarchy of ATP-consuming processes in mammalian cells. *Biochem J* **312 (Pt 1)**, 163-167, doi:10.1042/bj3120163 (1995).

4 Robichaud, N., Sonenberg, N., Ruggero, D. & Schneider, R. J. Translational Control in Cancer. *Cold Spring Harb Perspect Biol* **11**, doi:10.1101/cshperspect.a032896 (2019).

5 Browning, K. S. & Bailey-Serres, J. Mechanism of cytoplasmic mRNA translation. *Arabidopsis Book* **13**, e0176, doi:10.1199/tab.0176 (2015).

6 Merrick, W. C. & Pavitt, G. D. Protein Synthesis Initiation in Eukaryotic Cells. *Cold Spring Harb Perspect Biol* **10**, doi:10.1101/cshperspect.a033092 (2018).

7 Rowlands, A. G., Panniers, R. & Henshaw, E. C. The catalytic mechanism of guanine nucleotide exchange factor action and competitive inhibition by phosphorylated eukaryotic initiation factor 2. *J Biol Chem* **263**, 5526-5533 (1988).

8 Pakos-Zebrucka, K. *et al.* The integrated stress response. *EMBO Rep* **17**, 1374-1395, doi:10.15252/embr.201642195 (2016).

9 Sonenberg, N. & Hinnebusch, A. G. Regulation of translation initiation in eukaryotes: mechanisms and biological targets. *Cell* **136**, 731-745, doi:10.1016/j.cell.2009.01.042 (2009).

10 Galloway, A. & Cowling, V. H. mRNA cap regulation in mammalian cell function and fate. *Biochim Biophys Acta Gene Regul Mech* **1862**, 270-279, doi:10.1016/j.bbagrm.2018.09.011 (2019).

11 Prevot, D., Darlix, J. L. & Ohlmann, T. Conducting the initiation of protein synthesis: the role of eIF4G. *Biol Cell* **95**, 141-156, doi:10.1016/s0248-4900(03)00031-5 (2003).

12 Bhat, M. *et al.* Targeting the translation machinery in cancer. *Nat Rev Drug Discov* **14**, 261-278, doi:10.1038/nrd4505 (2015).

13 Sonenberg, N., Morgan, M. A., Merrick, W. C. & Shatkin, A. J. A polypeptide in eukaryotic initiation factors that crosslinks specifically to the 5'-terminal cap in mRNA. *Proc Natl Acad Sci U S A* **75**, 4843-4847, doi:10.1073/pnas.75.10.4843 (1978).

14 Altmann, M., Handschin, C. & Trachsel, H. mRNA cap-binding protein: cloning of the gene encoding protein synthesis initiation factor eIF-4E from Saccharomyces cerevisiae. *Mol Cell Biol* **7**, 998-1003, doi:10.1128/mcb.7.3.998-1003.1987 (1987).

15 Rychlik, W., Domier, L. L., Gardner, P. R., Hellmann, G. M. & Rhoads, R. E. Amino acid sequence of the mRNA cap-binding protein from human tissues. *Proc Natl Acad Sci U S A* **84**, 945-949, doi:10.1073/pnas.84.4.945 (1987).

16 Uttam, S., Wong, C., Price, T. J. & Khoutorsky, A. eIF4E-Dependent Translational Control: A Central Mechanism for Regulation of Pain Plasticity. *Front Genet* **9**, 470, doi:10.3389/fgene.2018.00470 (2018).

17 Raught, B. & Gingras, A. C. eIF4E activity is regulated at multiple levels. *Int J Biochem Cell B* **31**, 43-57, doi:Doi 10.1016/S1357-2725(98)00131-9 (1999).

18 Haghighat, A., Mader, S., Pause, A. & Sonenberg, N. Repression of cap-dependent translation by 4E-binding protein 1: competition with p220 for binding to eukaryotic

initiation factor-4E. *EMBO J* **14**, 5701-5709, doi:10.1002/j.1460-2075.1995.tb00257.x (1995).
19 Fadden, P., Haystead, T. A. J. & Lawrence, J. C. Identification of phosphorylation sites in the translational regulator, PHAS-I, that are controlled by insulin and rapamycin in rat adipocytes. *Journal of Biological Chemistry* **272**, 10240-10247 (1997).
20 Hay, N. & Sonenberg, N. Upstream and downstream of mTOR. *Genes Dev* **18**, 1926-1945, doi:10.1101/gad.1212704 (2004).
21 Lin, T. A. *et al.* PHAS-I as a link between mitogen-activated protein kinase and translation initiation. *Science* **266**, 653-656, doi:10.1126/science.7939721 (1994).
22 Pause, A. *et al.* Insulin-dependent stimulation of protein synthesis by phosphorylation of a regulator of 5'-cap function. *Nature* **371**, 762-767, doi:10.1038/371762a0 (1994).
23 Waskiewicz, A. J. *et al.* Phosphorylation of the cap-binding protein eukaryotic translation initiation factor 4E by protein kinase Mnk1 in vivo. *Mol Cell Biol* **19**, 1871-1880, doi:10.1128/MCB.19.3.1871 (1999).
24 Buxade, M., Parra-Palau, J. L. & Proud, C. G. The Mnks: MAP kinase-interacting kinases (MAP kinase signal-integrating kinases). *Front Biosci* **13**, 5359-5373, doi:10.2741/3086 (2008).
25 Fukunaga, R. & Hunter, T. MNK1, a new MAP kinase-activated protein kinase, isolated by a novel expression screening method for identifying protein kinase substrates. *EMBO J* **16**, 1921-1933, doi:10.1093/emboj/16.8.1921 (1997).
26 Waskiewicz, A. J., Flynn, A., Proud, C. G. & Cooper, J. A. Mitogen-activated protein kinases activate the serine/threonine kinases Mnk1 and Mnk2. *EMBO J* **16**, 1909-1920, doi:10.1093/emboj/16.8.1909 (1997).
27 Pyronnet, S. *et al.* Human eukaryotic translation initiation factor 4G (eIF4G) recruits mnk1 to phosphorylate eIF4E. *EMBO J* **18**, 270-279, doi:10.1093/emboj/18.1.270 (1999).
28 Furic, L. *et al.* eIF4E phosphorylation promotes tumorigenesis and is associated with prostate cancer progression. *Proc Natl Acad Sci U S A* **107**, 14134-14139, doi:10.1073/pnas.1005320107 (2010).
29 Ueda, T., Watanabe-Fukunaga, R., Fukuyama, H., Nagata, S. & Fukunaga, R. Mnk2 and Mnk1 are essential for constitutive and inducible phosphorylation of eukaryotic initiation factor 4E but not for cell growth or development. *Mol Cell Biol* **24**, 6539-6549, doi:10.1128/MCB.24.15.6539-6549.2004 (2004).
30 Jensen, K. B. *et al.* capCLIP: a new tool to probe translational control in human cells through capture and identification of the eIF4E-mRNA interactome. *Nucleic Acids Res* **49**, doi:ARTN e105
10.1093/nar/gkab604 (2021).
31 Scheper, G. C. *et al.* Phosphorylation of eukaryotic initiation factor 4E markedly reduces its affinity for capped mRNA. *J Biol Chem* **277**, 3303-3309, doi:10.1074/jbc.M103607200 (2002).
32 Slepenkov, S. V., Darzynkiewicz, E. & Rhoads, R. E. Stopped-flow kinetic analysis of eIF4E and phosphorylated eIF4E binding to cap analogs and capped oligoribonucleotides: evidence for a one-step binding mechanism. *J Biol Chem* **281**, 14927-14938, doi:10.1074/jbc.M601653200 (2006).
33 Zuberek, J. *et al.* Influence of electric charge variation at residues 209 and 159 on the interaction of eIF4E with the mRNA 5' terminus. *Biochemistry* **43**, 5370-5379, doi:10.1021/bi030266t (2004).

34 Prabhu, S. A., Moussa, O., Miller, W. H., Jr. & Del Rincon, S. V. The MNK1/2-eIF4E Axis as a Potential Therapeutic Target in Melanoma. *Int J Mol Sci* **21**, doi:10.3390/ijms21114055 (2020).
35 Silvera, D., Formenti, S. C. & Schneider, R. J. Translational control in cancer. *Nat Rev Cancer* **10**, 254-266, doi:10.1038/nrc2824 (2010).
36 Koromilas, A. E. Roles of the translation initiation factor eIF2alpha serine 51 phosphorylation in cancer formation and treatment. *Biochim Biophys Acta* **1849**, 871-880, doi:10.1016/j.bbagrm.2014.12.007 (2015).
37 Kim, S. H., Gunnery, S., Choe, J. K. & Mathews, M. B. Neoplastic progression in melanoma and colon cancer is associated with increased expression and activity of the interferon-inducible protein kinase, PKR. *Oncogene* **21**, 8741-8748, doi:10.1038/sj.onc.1205987 (2002).
38 Rosenwald, I. B., Wang, S., Savas, L., Woda, B. & Pullman, J. Expression of translation initiation factor eIF-2alpha is increased in benign and malignant melanocytic and colonic epithelial neoplasms. *Cancer* **98**, 1080-1088, doi:10.1002/cncr.11619 (2003).
39 Wang, S. *et al.* Expression of the eukaryotic translation initiation factors 4E and 2alpha in non-Hodgkin's lymphomas. *Am J Pathol* **155**, 247-255, doi:10.1016/s0002-9440(10)65118-8 (1999).
40 Robichaud, N. & Sonenberg, N. Translational control and the cancer cell response to stress. *Curr Opin Cell Biol* **45**, 102-109, doi:10.1016/j.ceb.2017.05.007 (2017).
41 Denoyelle, S. *et al.* In vitro inhibition of translation initiation by N,N'-diarylureas--potential anti-cancer agents. *Bioorg Med Chem Lett* **22**, 402-409, doi:10.1016/j.bmcl.2011.10.126 (2012).
42 Hamamura, K. *et al.* Attenuation of malignant phenotypes of breast cancer cells through eIF2alpha-mediated downregulation of Rac1 signaling. *Int J Oncol* **44**, 1980-1988, doi:10.3892/ijo.2014.2366 (2014).
43 Fukuchi-Shimogori, T. *et al.* Malignant transformation by overproduction of translation initiation factor eIF4G. *Cancer Res* **57**, 5041-5044 (1997).
44 Lazaris-Karatzas, A., Montine, K. S. & Sonenberg, N. Malignant transformation by a eukaryotic initiation factor subunit that binds to mRNA 5' cap. *Nature* **345**, 544-547, doi:10.1038/345544a0 (1990).
45 Ruggero, D. *et al.* The translation factor eIF-4E promotes tumor formation and cooperates with c-Myc in lymphomagenesis. *Nat Med* **10**, 484-486, doi:10.1038/nm1042 (2004).
46 Silvera, D. *et al.* Essential role for eIF4GI overexpression in the pathogenesis of inflammatory breast cancer. *Nat Cell Biol* **11**, 903-908, doi:10.1038/ncb1900 (2009).
47 Darveau, A., Pelletier, J. & Sonenberg, N. Differential efficiencies of in vitro translation of mouse c-myc transcripts differing in the 5' untranslated region. *Proc Natl Acad Sci U S A* **82**, 2315-2319, doi:10.1073/pnas.82.8.2315 (1985).
48 Rosenwald, I. B., Lazaris-Karatzas, A., Sonenberg, N. & Schmidt, E. V. Elevated levels of cyclin D1 protein in response to increased expression of eukaryotic initiation factor 4E. *Mol Cell Biol* **13**, 7358-7363, doi:10.1128/mcb.13.12.7358-7363.1993 (1993).
49 Ruggero, D. Translational control in cancer etiology. *Cold Spring Harb Perspect Biol* **5**, doi:10.1101/cshperspect.a012336 (2013).

50 Lin, C. J., Cencic, R., Mills, J. R., Robert, F. & Pelletier, J. c-Myc and eIF4F are components of a feedforward loop that links transcription and translation. *Cancer Res* **68**, 5326-5334, doi:10.1158/0008-5472.CAN-07-5876 (2008).
51 Kandoth, C. *et al.* Mutational landscape and significance across 12 major cancer types. *Nature* **502**, 333-339, doi:10.1038/nature12634 (2013).
52 Hsieh, A. C. *et al.* Genetic dissection of the oncogenic mTOR pathway reveals druggable addiction to translational control via 4EBP-eIF4E. *Cancer Cell* **17**, 249-261, doi:10.1016/j.ccr.2010.01.021 (2010).
53 Petroulakis, E. *et al.* p53-dependent translational control of senescence and transformation via 4E-BPs. *Cancer Cell* **16**, 439-446, doi:10.1016/j.ccr.2009.09.025 (2009).
54 Zoncu, R., Efeyan, A. & Sabatini, D. M. mTOR: from growth signal integration to cancer, diabetes and ageing. *Nat Rev Mol Cell Biol* **12**, 21-35, doi:10.1038/nrm3025 (2011).
55 Wendel, H. G. *et al.* Dissecting eIF4E action in tumorigenesis. *Genes Dev* **21**, 3232-3237, doi:10.1101/gad.1604407 (2007).
56 Chen, Y. T., Tsai, H. P., Wu, C. C., Wang, J. Y. & Chai, C. Y. Eukaryotic translation initiation factor 4E (eIF-4E) expressions are associated with poor prognosis in colorectal adenocarcinoma. *Pathol Res Pract* **213**, 490-495, doi:10.1016/j.prp.2017.02.004 (2017).
57 Graff, J. R. *et al.* eIF4E Activation Is Commonly Elevated in Advanced Human Prostate Cancers and Significantly Related to Reduced Patient Survival. *Cancer Research* **69**, 3866-3873, doi:10.1158/0008-5472.Can-08-3472 (2009).
58 Holm, N. *et al.* A prospective trial on initiation factor 4E (eIF4E) overexpression and cancer recurrence in node-negative breast cancer. *Ann Surg Oncol* **15**, 3207-3215, doi:10.1245/s10434-008-0086-9 (2008).
59 Khosravi, S. *et al.* eIF4E Is an Adverse Prognostic Marker of Melanoma Patient Survival by Increasing Melanoma Cell Invasion. *J Invest Dermatol* **135**, 1358-1367, doi:10.1038/jid.2014.552 (2015).
60 Carter, J. H. *et al.* Phosphorylation of eIF4E serine 209 is associated with tumour progression and reduced survival in malignant melanoma. *Brit J Cancer* **114**, 444-453, doi:10.1038/bjc.2015.450 (2016).
61 Fan, S. Q. *et al.* Phosphorylated eukaryotic translation initiation factor 4 (eIF4E) is elevated in human cancer tissues. *Cancer Biology & Therapy* **8**, 1463-1469, doi:DOI 10.4161/cbt.8.15.8960 (2009).
62 Robichaud, N. *et al.* Phosphorylation of eIF4E promotes EMT and metastasis via translational control of SNAIL and MMP-3. *Oncogene* **34**, 2032-2042, doi:10.1038/onc.2014.146 (2015).
63 Robichaud, N. *et al.* Translational control in the tumor microenvironment promotes lung metastasis: Phosphorylation of eIF4E in neutrophils. *Proc Natl Acad Sci U S A* **115**, E2202-E2209, doi:10.1073/pnas.1717439115 (2018).
64 Konicek, B. W. *et al.* Therapeutic inhibition of MAP kinase interacting kinase blocks eukaryotic initiation factor 4E phosphorylation and suppresses outgrowth of experimental lung metastases. *Cancer Res* **71**, 1849-1857, doi:10.1158/0008-5472.CAN-10-3298 (2011).
65 Suarez, M. *et al.* Inhibitory effects of Tomivosertib in acute myeloid leukemia. *Oncotarget* **12**, 955-966, doi:10.18632/oncotarget.27952 (2021).

66 Webster, K. R. *et al.* eFT508, a Potent and Selective Mitogen-Activated Protein Kinase Interacting Kinase (MNK) 1 and 2 Inhibitor, Is Efficacious in Preclinical Models of Diffuse Large B-Cell Lymphoma (DLBCL). *Blood* **126**, doi:DOI 10.1182/blood.V126.23.1554.1554 (2015).
67 Graff, J. R. *et al.* Therapeutic suppression of translation initiation factor eIF4E expression reduces tumor growth without toxicity. *Journal of Clinical Investigation* **117**, 2638-2648, doi:10.1172/Jci32044 (2007).
68 Wagner, C. R., Iyer, V. V. & McIntee, E. J. Pronucleotides: Toward the in vivo delivery of antiviral and anticancer nucleotides. *Med Res Rev* **20**, 417-451, doi:Doi 10.1002/1098-1128(200011)20:6<417::Aid-Med1>3.0.Co;2-Z (2000).
69 Li, S. *et al.* Treatment of breast and lung cancer cells with a N-7 benzyl guanosine monophosphate tryptamine phosphoramidate pronucleotide (4Ei-1) results in chemosensitization to gemcitabine and induced eIF4E proteasomal degradation. *Mol Pharm* **10**, 523-531, doi:10.1021/mp300699d (2013).
70 Moerke, N. J. *et al.* Small-molecule inhibition of the interaction between the translation initiation factors eIF4E and eIF4G. *Cell* **128**, 257-267, doi:10.1016/j.cell.2006.11.046 (2007).
71 Chen, L. *et al.* Tumor suppression by small molecule inhibitors of translation initiation. *Oncotarget* **3**, 869-881, doi:10.18632/oncotarget.598 (2012).
72 Bordeleau, M. E. *et al.* Functional characterization of IRESes by an inhibitor of the RNA helicase eIF4A. *Nat Chem Biol* **2**, 213-220, doi:10.1038/nchembio776 (2006).
73 Bordeleau, M. E. *et al.* Stimulation of mammalian translation initiation factor eIF4A activity by a small molecule inhibitor of eukaryotic translation. *Proc Natl Acad Sci U S A* **102**, 10460-10465, doi:10.1073/pnas.0504249102 (2005).
74 Cencic, R. *et al.* Antitumor Activity and Mechanism of Action of the Cyclopenta[b]benzofuran, Silvestrol. *Plos One* **4**, doi:ARTN e5223 10.1371/journal.pone.0005223 (2009).
75 Low, W. K. *et al.* Inhibition of eukaryotic translation initiation by the marine natural product pateamine A. *Mol Cell* **20**, 709-722, doi:10.1016/j.molcel.2005.10.008 (2005).
76 Tsumuraya, T. *et al.* Effects of hippuristanol, an inhibitor of eIF4A, on adult T-cell leukemia. *Biochem Pharmacol* **81**, 713-722, doi:10.1016/j.bcp.2010.12.025 (2011).
77 Vezina, C., Kudelski, A. & Sehgal, S. N. Rapamycin (Ay-22,989), a New Antifungal Antibiotic .1. Taxonomy of Producing Streptomycete and Isolation of Active Principle. *J Antibiot* **28**, 721-726, doi:DOI 10.7164/antibiotics.28.721 (1975).
78 Oshiro, N. *et al.* Dissociation of raptor from mTOR is a mechanism of rapamycin-induced inhibition of mTOR function. *Cell Struct Funct* **29**, 83-83 (2004).
79 Yip, C. K., Murata, K., Walz, T., Sabatini, D. M. & Kang, S. A. Structure of the Human mTOR Complex I and Its Implications for Rapamycin Inhibition. *Molecular Cell* **38**, 768-774, doi:10.1016/j.molcel.2010.05.017 (2010).
80 Tsukumo, Y., Alain, T., Fonseca, B. D., Nadon, R. & Sonenberg, N. Translation control during prolonged mTORC1 inhibition mediated by 4E-BP3. *Nat Commun* **7**, 11776, doi:10.1038/ncomms11776 (2016).
81 Kang, S. A. *et al.* mTORC1 Phosphorylation Sites Encode Their Sensitivity to Starvation and Rapamycin. *Science* **341**, 364-+, doi:ARTN 1236566 10.1126/science.1236566 (2013).

82 Feldman, M. E. *et al.* Active-Site Inhibitors of mTOR Target Rapamycin-Resistant Outputs of mTORC1 and mTORC2. *Plos Biol* **7**, 371-383, doi:ARTN e1000038 10.1371/journal.pbio.1000038 (2009).
83 Guichard, S. M. *et al.* AZD2014, an Inhibitor of mTORC1 and mTORC2, Is Highly Effective in ER+ Breast Cancer When Administered Using Intermittent or Continuous Schedules. *Molecular Cancer Therapeutics* **14**, 2508-2518, doi:10.1158/1535-7163.Mct-15-0365 (2015).
84 Thoreen, C. C. *et al.* An ATP-competitive Mammalian Target of Rapamycin Inhibitor Reveals Rapamycin-resistant Functions of mTORC1. *Journal of Biological Chemistry* **284**, 8023-8032, doi:10.1074/jbc.M900301200 (2009).
85 Janes, M. R. *et al.* Efficacy of the investigational mTOR kinase inhibitor MLN0128/INK128 in models of B-cell acute lymphoblastic leukemia. *Leukemia* **27**, 586-594, doi:10.1038/leu.2012.276 (2013).
86 Choo, A. Y. & Blenis, J. Not all substrates are treated equally Implications for mTOR, rapamycin-resistance and cancer therapy. *Cell Cycle* **8**, 567-572, doi:DOI 10.4161/cc.8.4.7659 (2009).
87 Carracedo, A. *et al.* Inhibition of mTORC1 leads to MAPK pathway activation through a PI3K-dependent feedback loop in human cancer. *Journal of Clinical Investigation* **118**, 3065-3074, doi:10.1172/jCI34739 (2008).
88 Bain, J. *et al.* The selectivity of protein kinase inhibitors: a further update. *Biochemical Journal* **408**, 297-315, doi:10.1042/Bj20070797 (2007).
89 Kannan, S. *et al.* Small Molecules Targeting the Inactive Form of the Mnk1/2 Kinases. *Acs Omega* **2**, 7881-7891, doi:10.1021/acsomega.7b01403 (2017).
90 Ramalingam, S. *et al.* The Novel Mnk1/2 Degrader and Apoptosis Inducer VNLG-152 Potently Inhibits TNBC Tumor Growth and Metastasis. *Cancers* **11**, doi:ARTN 299 10.3390/cancers11030299 (2019).
91 Reich, S. H. *et al.* Structure-based Design of Pyridone-Aminal eFT508 Targeting Dysregulated Translation by Selective Mitogen-activated Protein Kinase Interacting Kinases 1 and 2 (MNK1/2) Inhibition. *J Med Chem* **61**, 3516-3540, doi:10.1021/acs.jmedchem.7b01795 (2018).
92 Zhan, Y. *et al.* MNK1/2 inhibition limits oncogenicity and metastasis of KIT-mutant melanoma. *J Clin Invest* **127**, 4179-4192, doi:10.1172/JCI91258 (2017).
93 Huang, F. *et al.* Inhibiting the MNK1/2-eIF4E axis impairs melanoma phenotype switching and potentiates antitumor immune responses. *J Clin Invest* **131**, doi:10.1172/JCI140752 (2021).
94 Knight, J. R. P. *et al.* MNK Inhibition Sensitizes KRAS-Mutant Colorectal Cancer to mTORC1 Inhibition by Reducing eIF4E Phosphorylation and c-MYC Expression. *Cancer Discov* **11**, 1228-1247, doi:10.1158/2159-8290.CD-20-0652 (2021).
95 Martinez, A. *et al.* Phosphorylation of eIF4E Confers Resistance to Cellular Stress and DNA-Damaging Agents through an Interaction with 4E-T: A Rationale for Novel Therapeutic Approaches. *PLoS One* **10**, e0123352, doi:10.1371/journal.pone.0123352 (2015).
96 Geter, P. A. *et al.* Hyperactive mTOR and MNK1 phosphorylation of eIF4E confer tamoxifen resistance and estrogen independence through selective mRNA translation reprogramming. *Genes Dev* **31**, 2235-2249, doi:10.1101/gad.305631.117 (2017).

97 Yin, L., Duan, J. J., Bian, X. W. & Yu, S. C. Triple-negative breast cancer molecular subtyping and treatment progress. *Breast Cancer Res* **22**, 61, doi:10.1186/s13058-020-01296-5 (2020).
98 Yersal, O. & Barutca, S. Biological subtypes of breast cancer: Prognostic and therapeutic implications. *World J Clin Oncol* **5**, 412-424, doi:10.5306/wjco.v5.i3.412 (2014).
99 Schmid, P. *et al.* Atezolizumab plus nab-paclitaxel as first-line treatment for unresectable, locally advanced or metastatic triple-negative breast cancer (IMpassion130): updated efficacy results from a randomised, double-blind, placebo-controlled, phase 3 trial. *Lancet Oncol* **21**, 44-59, doi:10.1016/S1470-2045(19)30689-8 (2020).
100 Barchiesi, G. *et al.* Emerging Role of PARP Inhibitors in Metastatic Triple Negative Breast Cancer. Current Scenario and Future Perspectives. *Front Oncol* **11**, 769280, doi:10.3389/fonc.2021.769280 (2021).
101 Heinzel, A. *et al.* Synthetic lethality guiding selection of drug combinations in ovarian cancer. *PLoS One* **14**, e0210859, doi:10.1371/journal.pone.0210859 (2019).
102 Leary, M., Heerboth, S., Lapinska, K. & Sarkar, S. Sensitization of Drug Resistant Cancer Cells: A Matter of Combination Therapy. *Cancers (Basel)* **10**, doi:10.3390/cancers10120483 (2018).
103 Dziadkowiec, K. N., Gasiorowska, E., Nowak-Markwitz, E. & Jankowska, A. PARP inhibitors: review of mechanisms of action and BRCA1/2 mutation targeting. *Prz Menopauzalny* **15**, 215-219, doi:10.5114/pm.2016.65667 (2016).
104 Xue, Y. *et al.* CDK4/6 inhibitors target SMARCA4-determined cyclin D1 deficiency in hypercalcemic small cell carcinoma of the ovary. *Nat Commun* **10**, 558, doi:10.1038/s41467-018-06958-9 (2019).
105 Scott, S. C., Lee, S. S. & Abraham, J. Mechanisms of therapeutic CDK4/6 inhibition in breast cancer. *Semin Oncol* **44**, 385-394, doi:10.1053/j.seminoncol.2018.01.006 (2017).
106 Xue, Y. B. *et al.* SMARCA4 loss is synthetic lethal with CDK4/6 inhibition in non-small cell lung cancer. *Nature Communications* **10**, doi:ARTN 557
10.1038/s41467-019-08380-1 (2019).
107 Gurumurthy, C. B. *et al.* CRISPR: a versatile tool for both forward and reverse genetics research. *Hum Genet* **135**, 971-976, doi:10.1007/s00439-016-1704-4 (2016).
108 Shang, W., Wang, F., Fan, G. & Wang, H. Key elements for designing and performing a CRISPR/Cas9-based genetic screen. *J Genet Genomics* **44**, 439-449, doi:10.1016/j.jgg.2017.09.005 (2017).
109 Schuster, A. *et al.* RNAi/CRISPR Screens: from a Pool to a Valid Hit. *Trends Biotechnol* **37**, 38-55, doi:10.1016/j.tibtech.2018.08.002 (2019).
110 Sur, S. *et al.* A panel of isogenic human cancer cells suggests a therapeutic approach for cancers with inactivated p53. *Proc Natl Acad Sci U S A* **106**, 3964-3969, doi:10.1073/pnas.0813333106 (2009).
111 Haagensen, E. J. *et al.* Pre-clinical use of isogenic cell lines and tumours in vitro and in vivo for predictive biomarker discovery; impact of KRAS and PI3KCA mutation status on MEK inhibitor activity is model dependent. *Eur J Cancer* **56**, 69-76, doi:10.1016/j.ejca.2015.12.012 (2016).
112 Shen, J. P. & Ideker, T. Synthetic Lethal Networks for Precision Oncology: Promises and Pitfalls. *J Mol Biol* **430**, 2900-2912, doi:10.1016/j.jmb.2018.06.026 (2018).

113 Prahallad, A. *et al.* Unresponsiveness of colon cancer to BRAF(V600E) inhibition through feedback activation of EGFR. *Nature* **483**, 100-U146, doi:10.1038/nature10868 (2012).
114 Topatana, W. *et al.* Advances in synthetic lethality for cancer therapy: cellular mechanism and clinical translation. *J Hematol Oncol* **13**, 118, doi:10.1186/s13045-020-00956-5 (2020).
115 Aguirre, A. J. *et al.* Genomic Copy Number Dictates a Gene-Independent Cell Response to CRISPR/Cas9 Targeting. *Cancer Discov* **6**, 914-929, doi:10.1158/2159-8290.CD-16-0154 (2016).
116 Munoz, D. M. *et al.* CRISPR Screens Provide a Comprehensive Assessment of Cancer Vulnerabilities but Generate False-Positive Hits for Highly Amplified Genomic Regions. *Cancer Discov* **6**, 900-913, doi:10.1158/2159-8290.CD-16-0178 (2016).
117 So, R. W. L. *et al.* Application of CRISPR genetic screens to investigate neurological diseases. *Mol Neurodegener* **14**, 41, doi:10.1186/s13024-019-0343-3 (2019).
118 O'Neil, N. J., Bailey, M. L. & Hieter, P. Synthetic lethality and cancer. *Nat Rev Genet* **18**, 613-623, doi:10.1038/nrg.2017.47 (2017).
119 Kim, R. K. *et al.* Activation of KRAS promotes the mesenchymal features of basal-type breast cancer. *Exp Mol Med* **47**, e137, doi:10.1038/emm.2014.99 (2015).
120 Chan, K., Tong, A. H. Y., Brown, K. R., Mero, P. & Moffat, J. Pooled CRISPR-Based Genetic Screens in Mammalian Cells. *J Vis Exp*, doi:10.3791/59780 (2019).
121 Li, W. *et al.* MAGeCK enables robust identification of essential genes from genome-scale CRISPR/Cas9 knockout screens. *Genome Biol* **15**, 554, doi:10.1186/s13059-014-0554-4 (2014).
122 Vervoort, S. J. *et al.* The PP2A-Integrator-CDK9 axis fine-tunes transcription and can be targeted therapeutically in cancer. *Cell*, doi:https://doi.org/10.1016/j.cell.2021.04.022 (2021).
123 Rodriguez-Fernandez, L. *et al.* Isoform-specific function of calpains in cell adhesion disruption: studies in postlactational mammary gland and breast cancer. *Biochem J* **473**, 2893-2909, doi:10.1042/BCJ20160198 (2016).
124 Chuang, H. Y. *et al.* Aminopeptidase A initiates tumorigenesis and enhances tumor cell stemness via TWIST1 upregulation in colorectal cancer. *Oncotarget* **8**, 21266-21280, doi:10.18632/oncotarget.15072 (2017).
125 Banerjee, S. Aldo Keto Reductases AKR1B1 and AKR1B10 in Cancer: Molecular Mechanisms and Signaling Networks. *Adv Exp Med Biol*, doi:10.1007/5584_2021_634 (2021).
126 Guan, Y., Bhandari, A., Zhang, X. & Wang, O. Uridine phosphorylase 1 associates to biological and clinical significance in thyroid carcinoma cell lines. *J Cell Mol Med* **23**, 7438-7448, doi:10.1111/jcmm.14612 (2019).
127 Franken, N. A., Rodermond, H. M., Stap, J., Haveman, J. & van Bree, C. Clonogenic assay of cells in vitro. *Nat Protoc* **1**, 2315-2319, doi:10.1038/nprot.2006.339 (2006).
128 Klein, M. E., Kovatcheva, M., Davis, L. E., Tap, W. D. & Koff, A. CDK4/6 Inhibitors: The Mechanism of Action May Not Be as Simple as Once Thought. *Cancer Cell* **34**, 9-20, doi:10.1016/j.ccell.2018.03.023 (2018).
129 Prichard, M. N. & Shipman, C., Jr. A three-dimensional model to analyze drug-drug interactions. *Antiviral Res* **14**, 181-205, doi:10.1016/0166-3542(90)90001-n (1990).

130 Soica, C. *et al.* The synergistic biologic activity of oleanolic and ursolic acids in complex with hydroxypropyl-gamma-cyclodextrin. *Molecules* **19**, 4924-4940, doi:10.3390/molecules19044924 (2014).
131 Lord, C. J., Quinn, N. & Ryan, C. J. Integrative analysis of large-scale loss-of-function screens identifies robust cancer-associated genetic interactions. *Elife* **9**, doi:10.7554/eLife.58925 (2020).
132 Ryan, C. J., Bajrami, I. & Lord, C. J. Synthetic Lethality and Cancer - Penetrance as the Major Barrier. *Trends Cancer* **4**, 671-683, doi:10.1016/j.trecan.2018.08.003 (2018).
133 Adesso, L. *et al.* Gemcitabine triggers a pro-survival response in pancreatic cancer cells through activation of the MNK2/eIF4E pathway. *Oncogene* **32**, 2848-2857, doi:10.1038/onc.2012.306 (2013).
134 Liu, S., Zha, J. & Lei, M. Inhibiting ERK/Mnk/eIF4E broadly sensitizes ovarian cancer response to chemotherapy. *Clin Transl Oncol* **20**, 374-381, doi:10.1007/s12094-017-1724-0 (2018).
135 Pancholi, S. *et al.* Tumour kinome re-wiring governs resistance to palbociclib in oestrogen receptor positive breast cancers, highlighting new therapeutic modalities. *Oncogene* **39**, 4781-4797, doi:10.1038/s41388-020-1284-6 (2020).
136 Mitchell, D. C., Menon, A. & Garner, A. L. Chemoproteomic Profiling Uncovers CDK4-Mediated Phosphorylation of the Translational Suppressor 4E-BP1. *Cell Chem Biol* **26**, 980-990 e988, doi:10.1016/j.chembiol.2019.03.012 (2019).
137 Joshi, S. & Platanias, L. C. Mnk kinase pathway: Cellular functions and biological outcomes. *World J Biol Chem* **5**, 321-333, doi:10.4331/wjbc.v5.i3.321 (2014).
138 Sandeman, L. Y. *et al.* Disabling MNK protein kinases promotes oxidative metabolism and protects against diet-induced obesity. *Mol Metab* **42**, 101054, doi:10.1016/j.molmet.2020.101054 (2020).
139 Matsushita, N., Matsushita, S., Hirakawa, S. & Higashiyama, S. Doxycycline-dependent inducible and reversible RNA interference mediated by a single lentivirus vector. *Biosci Biotechnol Biochem* **77**, 776-781, doi:10.1271/bbb.120917 (2013).
140 Sanson, K. R. *et al.* Optimized libraries for CRISPR-Cas9 genetic screens with multiple modalities. *Nat Commun* **9**, 5416, doi:10.1038/s41467-018-07901-8 (2018).
141 Hart, T. *et al.* Evaluation and Design of Genome-Wide CRISPR/SpCas9 Knockout Screens. *G3 (Bethesda)* **7**, 2719-2727, doi:10.1534/g3.117.041277 (2017).
142 Sanjana, N. E., Shalem, O. & Zhang, F. Improved vectors and genome-wide libraries for CRISPR screening. *Nat Methods* **11**, 783-784, doi:10.1038/nmeth.3047 (2014).
143 de Weck, A. *et al.* Correction of copy number induced false positives in CRISPR screens. *PLoS Comput Biol* **14**, e1006279, doi:10.1371/journal.pcbi.1006279 (2018).
144 McGlincy, N. J. & Ingolia, N. T. Transcriptome-wide measurement of translation by ribosome profiling. *Methods* **126**, 112-129, doi:10.1016/j.ymeth.2017.05.028 (2017).
145 Guzman, C., Bagga, M., Kaur, A., Westermarck, J. & Abankwa, D. ColonyArea: an ImageJ plugin to automatically quantify colony formation in clonogenic assays. *PLoS One* **9**, e92444, doi:10.1371/journal.pone.0092444 (2014).